# Title: β-lactamase Amplification and Porin Loss Drive Progressive β-lactam Resistance in Recurrent ESBL *Enterobacteriaceae* Bacteremia

**Authors:** William C. Shropshire[1,2], Samuel L. Aitken[2,3], Reed Pifer[4], Jiwoong Kim[5], Micah M. Bhatti[6], Xiqi Li[7], Awdhesh Kalia[8], Jessica Galloway-Peña[2,7,9], Pranoti Sahasrabhojane[7], Cesar A. Arias[1,2,10,11], David E. Greenberg[2,12,13], Blake M. Hanson[1,2], Samuel A. Shelburne[2,7,9*]

**One Sentence Summary:** Amplification of β-lactam genes with porin loss was associated with development of β-lactam resistance in serial *Enterobacteriaceae* clinical isolates.

**Affiliations:**

[1] Center for Infectious Diseases, School of Public Health, University of Texas Health Science Center, Houston, TX, USA.

[2]Center for Antimicrobial Resistance and Microbial Genomics, Division of Infectious Diseases, University of Texas McGovern Medical School at Houston, Houston, TX, USA.

[3]Division of Pharmacy, MD Anderson Cancer Center, Houston, TX, USA.

[4]Division of Infectious Diseases, Department of Internal Medicine, University of Texas McGovern Medical School at Houston, Houston, TX, USA.

[5]Department of Bioinformatics, UT Southwestern Medical Center, Dallas TX, USA.

[6]Department of Laboratory Medicine, MD Anderson Cancer Center, Houston, TX, USA.

[7]Department of Infectious Diseases, MD Anderson Cancer Center, Houston TX, USA.

[8]Graduate Program in Diagnostic Genetics, School of Health Professions, The University of Texas M.D. Anderson Cancer Center, Houston, Texas, USA.

[9]Department of Genomic Medicine, MD Anderson Cancer Center, Houston TX, USA.

[10]Department of Microbiology and Molecular Genetics, University of Texas McGovern Medical School at Houston, Houston, TX, USA.

[11]Molecular Genetics and Antimicrobial Resistance Unit-International Center for Microbial Genomics, Universidad El Bosque, Bogota, Colombia.

[12]Department of Internal Medicine, UT Southwestern, Dallas, TX, USA.

[13]Department of Microbiology, UT Southwestern, Dallas, TX, USA.

*To whom correspondence should be addressed:

Samuel A. Shelburne, MD, PhD, sshelburne@mdanderson.org

## Abstract

Carbapenem resistant Enterobacteriaceae (CRE) are a critical public health issue. Recent studies indicate many CRE lack carbapenemases, but contain extended spectrum β-lactamases (ESBLs). We investigated 16 longitudinal, recurrent cases of extended spectrum B-lactamase (ESBL)-positive Enterobacteriaceae bacteremia to gain insights into mechanisms underlying the emergence of non-carbapenemase producing CRE (non-CP-CRE). Using a combination of short- and long-read sequencing technologies, we identified that non-CP-CRE emerges from an ESBL background through a combination of insertion sequence mediated β-lactamase translocation, subsequent amplification of β-lactamase encoding genes such as blaOXA-1 and blaCTX-M, and porin inactivation. Interestingly, the β-lactamase gene amplification occurred both on plasmids and on the chromosome, including in the middle of porin-encoding genes. Additionally, overexpression of blaOXA-1 increased resistance to the broad-spectrum β-lactam, piperacillin-tazobactam. This analysis shows mechanisms underlying non-CP-CRE emergence and demonstrates that copy number of β-lactamase genes needs to be considered to fully understand antimicrobial resistance amongst key human pathogens.

# Introduction

Antimicrobial resistance (AMR) is an emerging global health priority (*1*). Carbapenem resistant *Enterobacteriaceae* (CRE) are among the most serious AMR threats (*2, 3*). CRE can develop due to the presence of a carbapenem hydrolyzing enzyme (*i.e.*, a carbapenemase) as well as through decreased intracellular concentrations of carbapenems resulting from changes in outer membrane permeability or drug efflux (*4-6*). Although most CRE research has focused on carbapenemases such as *Klebsiella pneumoniae* carbapenemase (KPC) (*7*), a recent systematic survey of CRE in the United States identified a carbapenemase in less than 50% of CRE isolates suggesting that non-carbapenemase based mechanisms are major contributors to CRE (*8*).

*Escherichia coli* and *K. pneumoniae* account for the majority of non-carbapenemase producing CRE (non-CP-CRE) (*9-12*). Clinical non-CP-CRE isolates for both species generally have extended spectrum β-lactamases (ESBL) or AmpC-like enzymes as well as mutations that alter porin function (*13-17*). *In vitro* models of non-CP-CRE have shown that the presence of an ESBL or AmpC enzyme is critical to the subsequent development of carbapenem resistance as strains lacking such enzymes do not develop carbapenem resistance during serial passage (*12, 18*). However, it is becoming increasingly clear that both the presence as well as the copy number of β-lactamases have important impacts on β-lactam susceptibility (*19*). For example, increasing the expression of the non-carbapenemase β-lactamases TEM-1, OXA-1, and CTX-M-15 in an *E. coli* porin deficient strain increased carbapenem minimum inhibitory concentrations (MIC) (*18*), while serial passaging of an ESBL or AmpC-producing isolate in the presence of a carbapenem can result in amplification of plasmid-borne β-lactamase genes (*20*). It is thought that increased expression of an ESBL or AmpC enzyme with concomitant low carbapenem levels induced by porin inactivation results in sufficient carbapenem hydrolysis or carbapenem-trapping for ESBLs (*18*) and AmpC (*21*) respectively to render strains carbapenem-resistant (CR). Increased production of the narrow spectrum TEM β-lactamase has similarly been reported to result in cefepime (*22*) and piperacillin-

tazobactam resistance (*23*), indicating that the effects of β-lactamase gene dosage are not limited to carbapenems.

The paucity of serially collected, clinical *Enterobacteriaceae* with an ESBL (ESBL-E) that are initially carbapenem sensitive, which develop a subsequent carbapenem resistant phenotype indicates that it is not clear whether the clinical development of carbapenem resistance in an ESBL-E strain mirrors that of laboratory conditions (*15, 24-27*). Several studies of serial, clinical *E. coli* strains expressing a $bla_{CMY}$ variant that produces an AmpC β-lactamase have shown that clinical non-CP-CRE isolates contain inactivated porins relative to their carbapenem-susceptible precursors; however, these studies did not examine $bla_{CMY}$ gene amplification (*24-26*). Furthermore, the vast majority of clinical non-CP-CRE harbor CTX-M β-lactamases (*14, 16, 28, 29*), and much less is known about how carbapenem resistance develops in such isolates.

Recently, whole genome sequencing (WGS) of a pair of *E. coli* isolates containing the ESBL gene, $bla_{CTX\text{-}M\text{-}15}$, identified that a single amino acid change in the OmpR protein, which regulates production of porins known as outer membrane protein C (OmpC) and OmpF, resulted in development of carbapenem resistance; however, no information was provided regarding $bla_{CTX\text{-}M}$ copy numbers in the genome (*15*). We recently identified that the vast majority of *Enterobacteriaceae* isolates resistant to 3$^{rd}$ generation cephalosporins at our institution contain $bla_{CTX\text{-}M}$ (*30*). Moreover, short-read Illumina WGS revealed high level read mapping to β-lactamase encoding genes in numerous isolates suggestive of ESBL gene amplification (*30*). Herein, we sought to determine the frequency in which CRE emerges following ESBL-E bacteremia at an institution with high rates of $bla_{CTX\text{-}M}$ harboring isolates and to determine the molecular mechanisms of carbapenem resistance using WGS of serial infecting strains.

# Results

## Patient population characteristics

A total of 116 patients (57% male, median age 59 years) with ESBL-E bacteremia were identified. *E. coli* was the most common organism (85%), followed by *K. pneumoniae* (13%), and *K. oxytoca* (2%). 42% of patients had leukemia and 49% were neutropenic at the time of index culture. 92% of patients received treatment with a carbapenem. Recurrent bacteremia was identified in 16 (14%) patients (*E. coli* [n=14], *K. pneumoniae* [n=2]) and occurred primarily in patients with leukemia (n = 12) or recipients of hematopoietic stem cell transplants (HSCT; n = 2). 4/16 (25%) patients with recurrent bacteremia had CR isolates. All four patients with CR isolates were infected with *E. coli* and had leukemia. Additional clinical data is presented in Table S1 and the Supplemental Material (Clinical Summary). The full set of serial isolates was available for 11/16 patients, including the four patients with a CR phenotype in a recurrent isolate.

## Assessment of clonality amongst the recurrent isolates

The 11 sets of temporally collected isolates, nine of which were *E. coli* and two were *K. pneumoniae*, contained a total of 26 strains. Eight patients had two bacteremia episodes, two patients had three episodes, and one had four episodes (Fig. 1). The initial isolates by definition had an ESBL phenotype; however, we observed a broad range of subsequent phenotypes in the serial strains. We noted in particular the loss of a resistant phenotype (n=2), ESBL persistence (n=5), and development of CR (n=4). One of four serial CRE strains isolated after the index ESBL strain indicated carbapenemase production by Carba-NP whereas the other three were non-CP-CRE (Fig. 1A). Our HiSeq WGS data analysis indicated seven patients had evidence of serial infection by highly similar strains whereas four were infected with a different strain (Fig. S1). The two sets of serial isolates which lost their respective AMR phenotypes (patient 2 and 5) notably did not cluster within the ML phylogenetic tree nor did they have the same MLST designation as their respective index strains. Similarly, the sole carbapenemase producing

organism was different from the index ESBL-E strain (patient 7). Conversely, in the three instances where the subsequent isolates were non-CP-CRE (patient 4, 10, and 11), all of the isolates from each patient clustered tightly together within the phylogenetic tree, had the same hierarchical population structure as determined using hierBAPS, and same MLST designation, thus indicating likely repeated infection from the same index strain (Fig. S1).

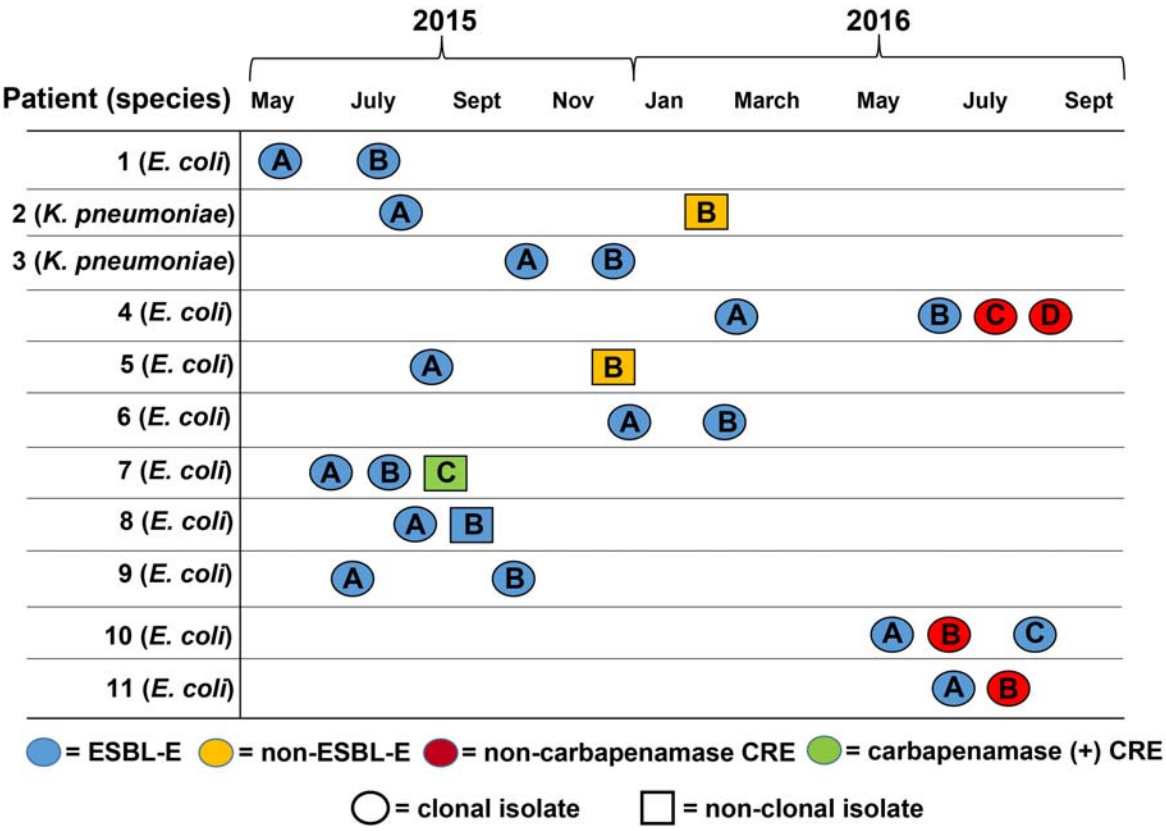


**Fig. 1. Overview of strains and assessment of strain clonality.** Time line showing date of serial isolation of same species from blood cultures. Patient numbers are in the first column. The shape and color of the isolates as labelled in the legend indicate clonality and antimicrobial resistance respectively. Patient subgroups (e.g. Patient 1; isolate A and B) refers to the order of isolation. Abbreviations are as follows: ESBL-E = extended spectrum β-lactamase producing *Enterobacteriaceae*, CRE = carbapenem resistant *Enterobacteriaceae*.

## Diversity of β-lactamase encoding AMR genes present in our cohort

A summary of the sequence types and identified β-lactamase encoding genes for the sequenced strains are presented in Table 1. Consistent with our previous data (*30*), all initial ESBL-E strains contained $bla_{\text{CTX-M}}$ with a variety of additional β-lactamase-encoding genes present in the various strains such as $bla_{\text{OXA}}$, $bla_{\text{SHV}}$, and $bla_{\text{TEM}}$ variants. The combination of $bla_{\text{OXA-1}}$ and $bla_{\text{CTX-M}}$ was particularly prevalent, being present in 12/26 isolates (46%). We only identified a single instance in which a serial clonal isolate acquired or lost a β-lactamase gene. This gain/loss event occurred within patient 7 and involved the gain of $bla_{\text{OXA-1}}$ and loss of $bla_{\text{SHV}}$ by isolate B relative to the index isolate A. In addition to assessing AMR gene presence, we also used the short-read data to assess read mapping depth and found that 12/26 strains had significantly increased mapping depth for β-lactamase-encoding genes including $bla_{\text{OXA}}$, $bla_{\text{CTX-M}}$, and $bla_{\text{TEM}}$ (Table 1). Interestingly, all of the serial isolates which developed non-CP-CRE phenotypes (patient 4, 10, and 11) had increased mapping depth for β-lactamase genes. Taken together with our clonality analyses, these data show that no index ESBL isolates developed CRE through carbapenemase acquisition and suggest that β-lactamase encoding gene amplification might contribute to the emergence of non-CP-CRE in our cohort.

## Consistent identification of porin loss with emergence of carbapenem resistance amongst non-CP-CRE isolates

When using the short-read data to compare the serial, clonal isolates that developed CR, the only consistently identified variation in the non-CP-CRE strains relative to their ESBL progenitors were inactivating mutations in the genes encoding the key porin proteins OmpC and OmpF. For *ompC* we observed an insertion sequence (IS) disruption as well as frame-shift inducing nucleotide deletions, whereas for *ompF*, we consistently found frame-shift inducing deletions (Fig. 2). No changes were identified in the *ompR* gene, which had previously been found in a single *E. coli* isolate that progressed from ESBL-E to non-CP-CRE and is a common mutation hotspot during *in vitro* CRE development (*15,*

*18*, *20*). For patient 10, we observed that isolate C (ESBL-E phenotype) contained identical wild-type *ompC* and *ompF* sequences as did the parent isolate, isolate A (ESBL-E phenotype), in contrast to isolate B (non-CP-CRE phenotype) in which *ompC* and *ompF* were interrupted by a 16 bp and an 11 bp deletion, respectively. For patient 11, *ompF* was mutated in both the initial isolate A (ESBL-E phenotype) and subsequent isolate B (non-CP-CRE phenotype) whereas *ompC* was only mutated (2 bp deletion) in the subsequent isolate B, non-CP-CRE strain.

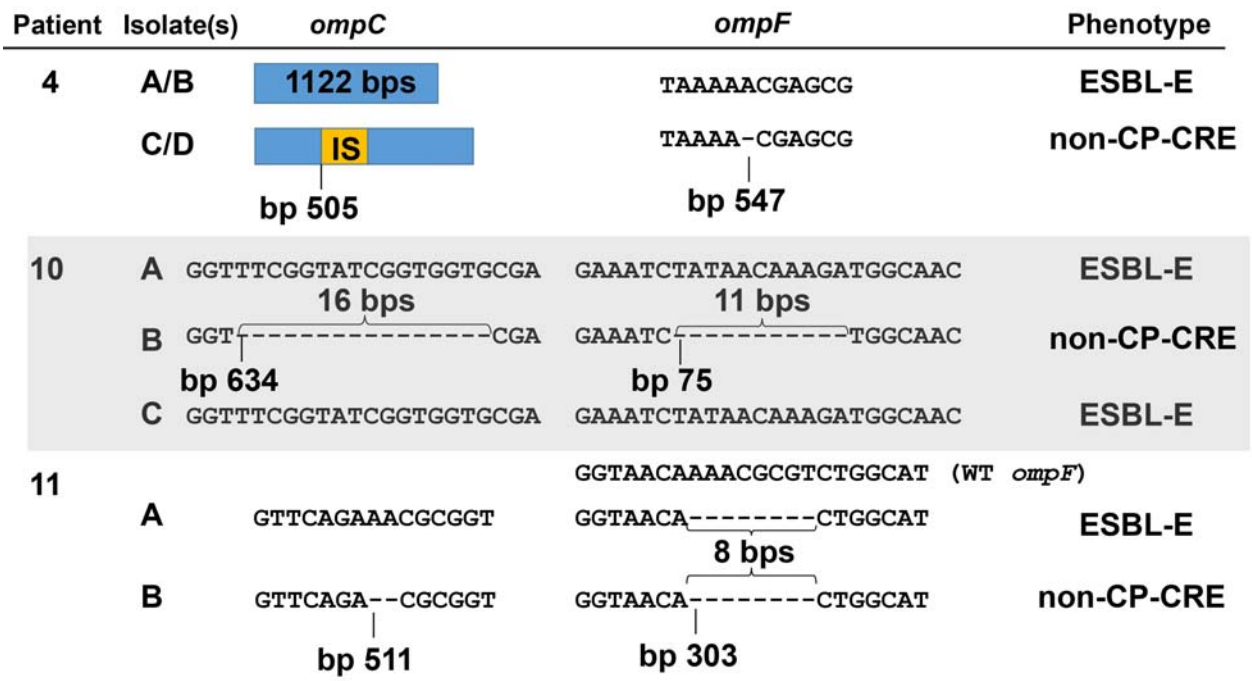


**Fig. 2. Delineation of changes in the porin encoding genes *ompC* and *ompF* in clonal serial isolates that developed carbapenem resistance using short-read data.** Shown are variations in *ompC* and *ompF* genes. For isolates C and D from patient 4, an insertion sequence (IS) interrupts the *ompC* open reading frame. For the remainder of the gene changes, we observed deletions that resulted in frame shifts. The location and extent of the deletions are labeled. For patient 11, both isolate A and B had deletions in *ompF* relative to wild-type, such that the *ompF* sequence from the *E. coli* reference strain MG1655 is shown for reference purposes. The corresponding phenotype is abbreviated as follows: ESBL-E = extended spectrum β-lactamase producing *Enterobacteriaceae*, non-CP-CRE = non-carbapenemase producing carbapenem-resistant *Enterobacteriaceae*.

## Characterization of β-lactamases in index ESBL isolates that developed carbapenem resistance

Given that the short-read data alone does not allow for creating consensus assemblies, we performed Oxford Nanopore Technology (ONT) sequencing on all index isolates that developed non-CP-CR (*i.e.* isolates from patients 4, 10, and 11) to fully characterize their respective genome structures. This approach allowed us to identify that MB1860 (isolate A, patient 4; ST131) and EC215 (isolate A, patient 10; ST131) both contain an approximately 8.1 kbp Translocatable Unit (TU), designated as MB1860TU, which is IS26-flanked, carries $bla_{\text{OXA-1}}$, and inserts adjacent to an IS26 element upstream of $bla_{\text{CTX-M-15}}$ (Fig. 3A).

When moving from the 5' to 3' end of MB1860TU on the MB1860 chromosome, IS26, an IS6 family insertion sequence, is located at the beginning of the TU structure. The downstream $bla_{\text{OXA-1}}$ gene is flanked by an aminoglycoside acetyltransferase, *aac(6')-Ib-cr*, and a truncated chloramphenicol resistance determinant (*⊿catB3*). A second aminoglycoside resistance determinant, *aac(3')-IIa*, and the tunicamycin resistance gene, *tmrB*, are separated from *aac(6')-Ib-cr*, $bla_{\text{OXA-1}}$, and *⊿catB3* by an IS6 element. These genes are followed by a region that includes an incomplete IS3 transposase, IS26, and a truncated Tn2 transposon, which signifies the end of the TU structure. MB1860TU is inserted adjacent to an IS26 element that is recombined with another truncated Tn2 transposon upstream of $bla_{\text{CTX-M-15}}$ and a final IS6 element. Similar IS26/Tn3 family transposable elements that have putatively formed via homologous recombination events have previously been reported in association with IS26-mediated AMR transfer in *Enterobacteriaceae* (*18*, *31*, *32*). MB1860TU was inserted into the MB1860 chromosome between *cirA*, which encodes for the Colicin I receptor, and a hypothetical protein (Fig. 3A).

The index isolate A for patient 11 (EC215) had almost an identical TU structure (coverage: 100%; BLAST identity: 99.9%) as MB1860TU inserted chromosomally within a similar region; however, the

TU is in a flipped orientation relative to the normalized start position of the chromosome (Fig. S2A). EC215 also contained a 180 kbp IncF plasmid that carries a modified MB1860TU (88% coverage; 99.9% BLAST ID) that lacks a recombined, truncated Tn2 transposon (purple brackets, Fig.S2B). It should be noted as well that the plasmid-encoded $bla_{\text{CTX-M-15}}$ and $bla_{\text{OXA-1}}$ genes are in differing orientations and spatially located further apart from one another as compared to the chromosomal copies of the genes suggesting independent translocation of each respective gene from plasmid to the chromosome.

The index isolate A for patient 10 (MB2315) did not carry any $bla_{\text{OXA-1}}$ gene copies nor any individual copies of $bla_{\text{CTX-M-15.}}$ In contrast, this isolate had a single copy of an ISEcp1/IS26-mediated TU carrying $bla_{\text{CTX-M-55}}$ located on a 142 kbp IncF plasmid which will be fully described in proceeding sections.

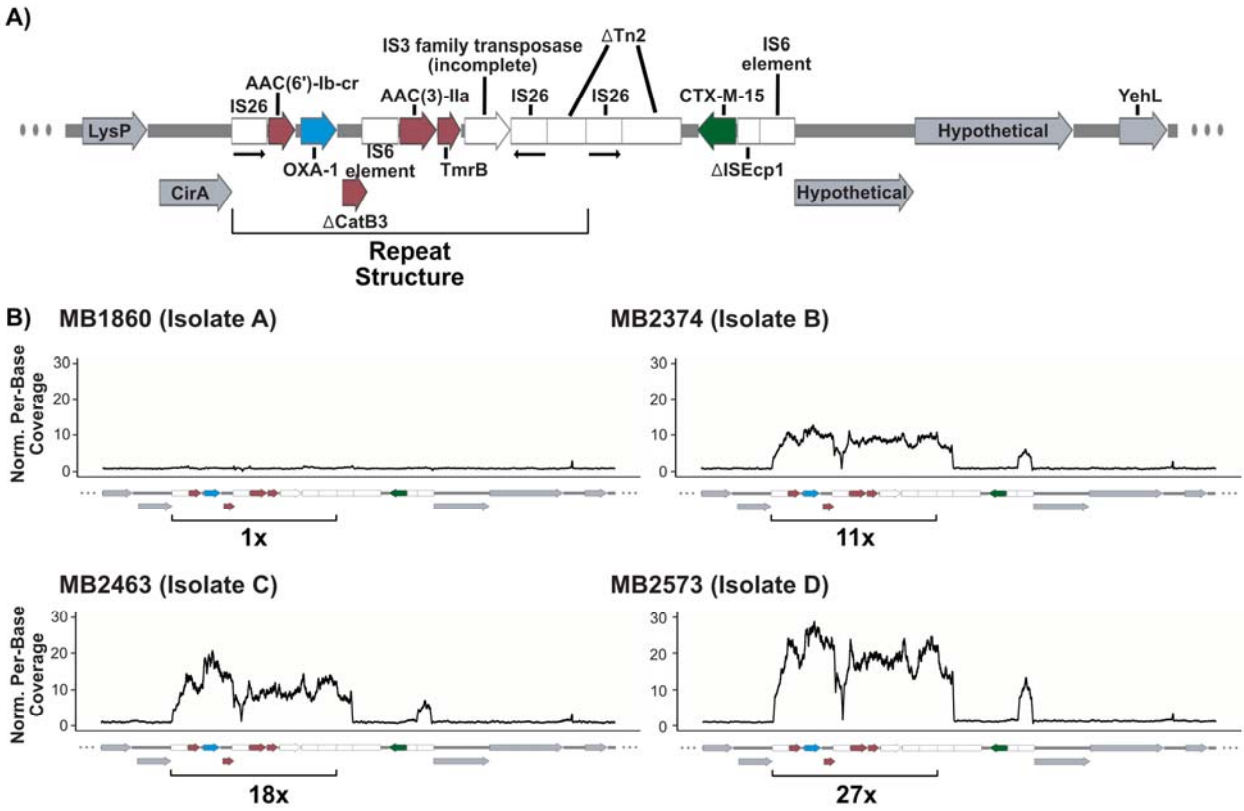


**Fig. 3. Translocatable unit MB1860TU characterization of patient 4 isolates with noted increase of WGS per-base coverage amongst serial isolates. (A)** Map of MB1860TU noted in black brackets identified from the initial ESBL isolate of patient 4 (MB1860). ORFs and MGEs are indicated by colored arrows and boxes with mobile genetic elements (white), AMR determinants (maroon), and other genes (gray) labelled respectively. Delta (Δ) next to annotated genetic region indicates a truncation or disruption. Black arrows beneath IS26 elements indicate directionality of IS26 transposases. *bla*$_{OXA-1}$ (blue) carried by MB1860TU is upstream of *bla*$_{CTX-M-15}$ (green). **(B)** Increasing coverage depth of MB1860TU for patient 4 serial isolates MB1860 (1X), MB2374 (11X), MB2463 (18X), and MB2573 (27X) respectively. MB1860TU mean coverage depth was normalized to the mean coverage depth for ST131 housekeeping genes.

## Delineation of genetic context of increased mapping depth for β-lactamase encoding genes

As previously noted, nearly half of the strains in our cohort, including all serial non-CP-CRE isolates, had increased read mapping depth for β-lactamase encoding genes (Table 1). Nevertheless, we could not use the short-read data alone to determine the gene amplification mechanism. Thus, we mapped the serial short-read data to assembled consensus genomes of the index isolates. We observed progressive increase in mapping depth for the serial isolates of patient 4 (strains MB1860-2573) up to 27-fold for $bla_{\text{OXA-1}}$ from the initial to final isolate (Fig. 3B). The increase in mapping depth did not extend to the nearby $bla_{\text{CTX-M-15}}$ gene but rather was confined to the MB1860TU region that contained *aac-(6')-Ib-cr,* $bla_{\text{OXA-1}}$, *ΔcatB3*, *aac(3')-IIa,* and *tmrB* (Fig. 3B). Patient 10 (strains MB2315-2446-2649) had increased mapping depth of $bla_{\text{CTX-M-55}}$ of ~2X fold for isolate B (MB2446) and ~7X fold for isolate C (MB2649). This isolate carried an IS*Ecp1*-$bla_{\text{CTX-M-55}}$-IS*26* 4.5 kbp TU, which appeared through the short-read data to be the element that was being amplified and will be discussed in detail below. Patient 11 serial isolates, EC215 (isolate A) and MB2489 (isolate B), both had the presence of two copies of $bla_{\text{OXA-1}}$and $bla_{\text{CTX-M-15}}$, one on a chromosome and one on a plasmid as previously mentioned. Nevertheless, no further increased mapping was detected between the original and serial isolate. We confirmed that the gene mapping depth observed by sequencing correlated with gene levels as measured by qRT-PCR (Fig. S3).

In order to determine whether the increases in gene mapping depth was associated with augmented transcript levels of the β-lactamase encoding genes, we isolated RNA, converted to cDNA, and then performed TaqMan qRT-PCR for $bla_{\text{OXA}}$ and $bla_{\text{CTX-M}}$ relative to the endogenous control gene *rpsL*. We observed in patient 4 isolates a statistically significant increase in $bla_{\text{OXA-1,}}$ but not $bla_{\text{CTX-M}}$ transcript levels in the serial isolates as compared to the index isolate that was consistent with read mapping depth data (Fig. 4A). The $bla_{\text{CTX-M}}$ transcript levels were only measured in patient 10 since $bla_{\text{OXA-1}}$ was not present in these strains. We observed a significant increase in $bla_{\text{CTX-M}}$ transcript levels for the second

and third isolate of patient 10 (Fig. 4B). No statistically significant differences were observed in either *bla*$_{\text{OXA-1}}$ or *bla*$_{\text{CTX-M}}$ transcript levels for either isolate from patient 11, which is in accordance with the stable gene mapping depth data observed in these isolates (Fig. 4C).

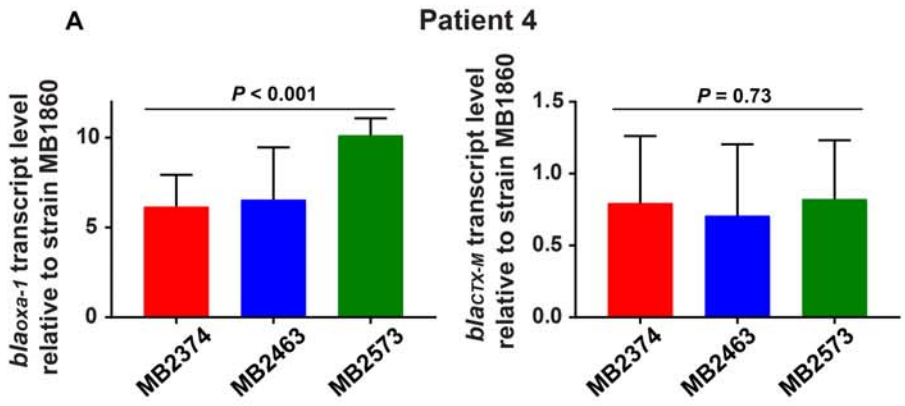


| Strain | TZP MIC | ERT MIC | $bla_{OXA-1}$ Depth | $bla_{CTX-M-15}$ Depth | OmpC Intact | OmpF Intact |
|---|---|---|---|---|---|---|
| 1860 (A) | 8 | ≤ 0.5 | 1.0 | 0.82 | Yes | Yes |
| 2374 (B) | ≥ 128 | ≤ 0.5 | 10.1 | 0.85 | Yes | Yes |
| 2463 (C) | ≥ 128 | ≥ 32 | 16.7 | 0.82 | No | No |
| 2573 (D) | ≥ 128 | ≥ 32 | 26.2 | 1.16 | No | No |

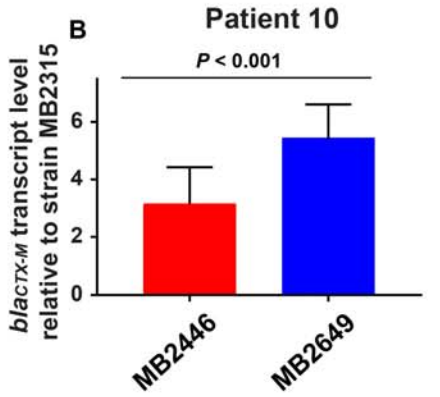


| Strain | TZP MIC | ERT MIC | CEP MIC | $bla_{CTX-M-55}$ Depth | OmpC Intact | OmpF Intact |
|---|---|---|---|---|---|---|
| 2315 (A) | 8 | ≤ 0.5 | 2 | 1.21 | Yes | Yes |
| 2446 (B) | ≥ 128 | ≥ 32 | ≥ 64 | 1.42 | No | No |
| 2649 (C) | 16 | ≤ 0.5 | ≥ 64 | 5.78 | Yes | Yes |

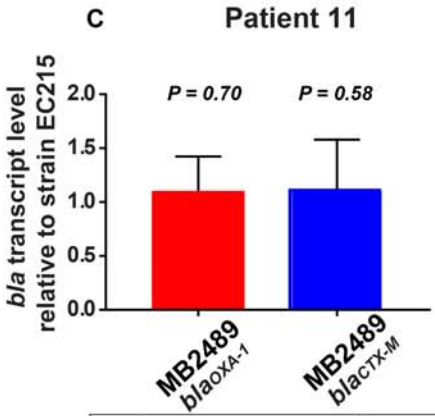


| Strain | TZP MIC | ERT MIC | $bla_{OXA-1}$ Depth | $bla_{CTX-M-15}$ Depth | OmpC Intact | OmpF Intact |
|---|---|---|---|---|---|---|
| EC215 (A) | 64 | ≤ 0.5 | 2.75 | 2.09 | Yes | No |
| 2489 (B) | ≥ 128 | ≥ 32 | 3.24 | 2.15 | No | No |

**Fig. 4. Analysis of β-lactamase gene transcript levels using qRT-PCR.** RNA was obtained from strains grown to mid-exponential phase in triplicate on two separate days (n = 6), converted to cDNA, and analyzed using TaqMan real-time QRT. Shown are mean transcript levels ± standard deviation of indicated genes relative to the index strains. β-lactamase gene transcript levels were normalized to the endogenous *rpsL* transcript levels. *P* values refer to Kruskall-Wallis test (panels A and B) and Wilcoxon Rank-sum test (panel C) for the serial isolates relative to the initial isolate. A summary of select antimicrobial MICs, read mapping depth via short-read sequencing, and porin status is provided for each patient to assist with visualization of relationship between the latter two factors and antimicrobial susceptibility. Abbreviations are as follows: TZP = piperacillin-tazobactam, ERT = ertapenem, and CEP = cefepime.

## Use of ONT Data to Visualize β-lactamase Gene Amplification and ORF Insertion

The gene mapping and qRT-PCR data strongly suggested gene amplification, but the highly repetitive nature of the mobile genetic elements (MGEs) did not allow for direct visualization using the short-read data. Thus, we performed ONT sequencing for all serial isolates and used the subsequent assemblies as well as individual long reads to look for the genetic context of the TUs and to determine how many TU copies were present in each isolate.

Fig. 5A shows MB1860TU plus ~60 kbp flanking regions of isolate MB1860 (isolate A, patient 4), which include the *ompC* gene 5' and *thidD-hypothetical-yvoA* gene region 3' in relation to the MB1860TU initial insertion site. When comparing the index isolate with serial isolates of patient 4, we consistently identified multiple, contiguous copies of the *aac-(6')-Ib', bla*$_{\text{OXA-1}}$, Δ*catB3*, *aac(3')-IIc,* and *tmrB* AMR encoding genes in conjunction with IS6 elements, which corresponds with our short-read mapping depth results indicating gene amplification (Fig. 5B). For strain MB2374 (isolate B), there were multiple reads that had 2X or greater copies of MB1860TU including one 31.5 kb ONT read which captured three contiguous repeats. We could determine through an alignment of the MB2374 long-reads with our reference chromosome MB1860 using an in-house developed tool called SVAnts in conjunction with a short-read pileup analysis that this 10X TU amplification only occurred at the original MB1860TU locus. As well as having TU amplification at the original MB1860TU site, additional gene amplification in the non-CP-CRE strains MB2463 (isolate C) and MB2649 (isolate D) resulted from the translocation and insertion of MB1860TU into the aforementioned flanking regions (Fig. 5B). Remarkably, the *ompC* disruption found in the short-read data analysis (Fig. 2) for the non-CP-CRE strains MB2463 (isolate C) and MB2649 (isolate D) resulted from the translocation and insertion of MB1860TU within the *ompC* gene (Fig. 5B). This *ompC* gene disruption was confirmed through the identification of multiple long-reads that covered the full insertion (>30 kbp) site as well as identifying partial assemblies of this insertion on individual contigs. We found two individual long reads that were able to span the full length of the MB1860TU array (3X copies) which disrupts *ompC* for isolate MB2463 (isolate C) and confirmed

the exact MB1860TU insertion location within *ompC* (c.504_505ins). We could not identify individual long reads that spanned the entire *ompC* insertion site in MB2649 (isolate D); however, the same genetic context that confirmed translocation and interruption of *ompC* was detected in individual long reads at the 5' and 3' regions of the *ompC* insertion site respectively. Additionally, a second MB1860TU translocation and insertion downstream of the original MB1860TU locus occurred in strain MB2649 (isolate D) within a hypothetical protein which resides between flanking genes *thiD* encoding a kinase and the HTH-type transcriptional repressor gene *yvoA* (Fig. 5B). This progressive amplification was consistent with our qRT-PCR data (Fig. S3A, Fig. 4A).

The serial isolates from patient 10 (MB2315, MB2446, and MB2649) contain a different TU and gene amplification mechanism compared to patient 4 isolates (Fig. 6). MB2315 (isolate A) harbors $bla_{\text{CTX-M-55}}$ located between IS*Ecp1* and an IS26 element, designated as MB2315TU, on a 141 kbp IncF conjugative plasmid. There are three additional small plasmids present in MB2315, one of which is a high copy number (~6X) 6.8 kbp plasmid that had 100% coverage, 100% BLAST ID with an *E. coli* plasmid identified as p7 from an unpublished collection in the UK (GenBank Accession #: CP023375). The p7 plasmid contains a small *sul2-Δaph(3")-Ib-dfrA14-Δaph(3")-Ib-aph(6')-Id* resistance island. MB2446 (isolate B) also carries MB2315TU on a similar IncF plasmid compared to the index strain. Additionally, in MB2446 the IncF plasmid-encoded MB2315TU translocates and inserts within the p7 plasmid in between *dfrA14* and *Δaph(3")-Ib* to generate three copies of MB2315TU , thereby creating a 19 kbp plasmid that reverts to a low copy (1X) number plasmid. In MB2649 (isolate C) $bla_{\text{CTX-M-55}}$ is on the same IncF plasmid as MB2446 (100%cov;99.99%ID) as well as the p7 plasmid; however, there is just a single IS*Ecp1*-$bla_{\text{CTX-M-55}}$ element on the p7 plasmid that has dropped IS26 from the full length MB2315TU. Interestingly, the MB2649 p7 plasmid reverts back to a high (6X) copy number plasmid with 1X copies of $bla_{\text{CTX-M-55}}$ suggesting that this configuration of the MB2315TU is more stable within this p7 plasmid.

These data are consistent with our qRT-PCR analysis where there is progressively higher DNA and transcript levels of $bla_{\text{CTX-M-55}}$ for each serial isolate (Fig. S3B, Fig. 4B).

Both isolates of patient 11 (EC215 and MB2489) had two copies of $bla_{CTX\text{-}M\text{-}15}$ and $bla_{OXA\text{-}1}$ on the MB1860TU-like structures located on the chromosome (Fig. S2A) and an IncFIB conjugative plasmid respectively (Fig. S2B), as previously described in the index isolate section. Consistent with our previous qRT-PCR (Fig.S3C, Fig. 4C), there was no indication in the ONT data of additional gene amplification via the MB1860TU occurring in this set of serial isolates.

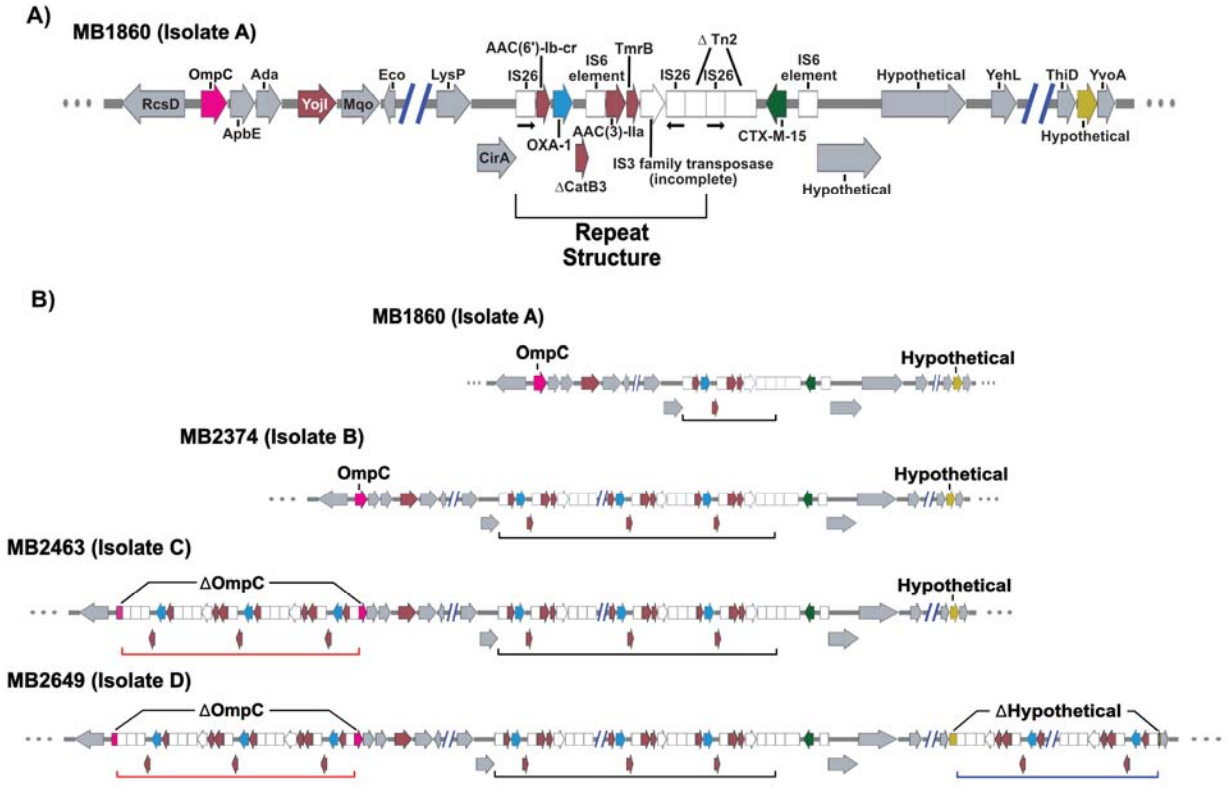


**Fig. 5. MB1860TU amplification and translocation into *ompC* and hypothetical proteins within patient 4 serial isolates. (A)** Genomic characterization of the region in which the IS26-mediated MB1860TU amplified and inserted with each subsequent serial isolate. ORFs are indicated by arrows with MGEs (white), AMR determinants (maroon), and other genes (gray) labelled respectively. Genes of particular interest: *ompC* (pink), $bla_{\text{OXA-1}}$ (blue), $bla_{\text{CTX-M-15}}$ (green), and a hypothetical protein gene (gold) are colored respectively. Black arrows beneath IS26 elements indicate directionality of IS26 transposases. Delta (Δ) next to annotated genetic region indicates a truncation or disruption. The 5' region including 5'-*ompC-apbE-ada-yojI-mqo-eco*-3' is ~65 kbp 5' to the region where the initial MB1860TU is located in MB1860. Furthermore, the 3' region is defined by 5'-*thiD-hyp-yvoA*-3' and located ~65 kbp from the initial MB1860TU region. In lieu of annotating the full region, these regions are omitted and indicated by blue dashes. **(B)** ONT sequencing assemblies and SVAnts long-read characterization of TU amplification

and insertion in serial isolates MB1860, MB2374, MB2463, and MB2649. Note that the insertion and disruption of *ompC* by MB1860TU is observed first in MB2463 (isolate C; red brackets) and persists in MB2649 (isolate D; red brackets) with an additional insertion and disruption into a hypothetical ORF in the 3' region (blue brackets).

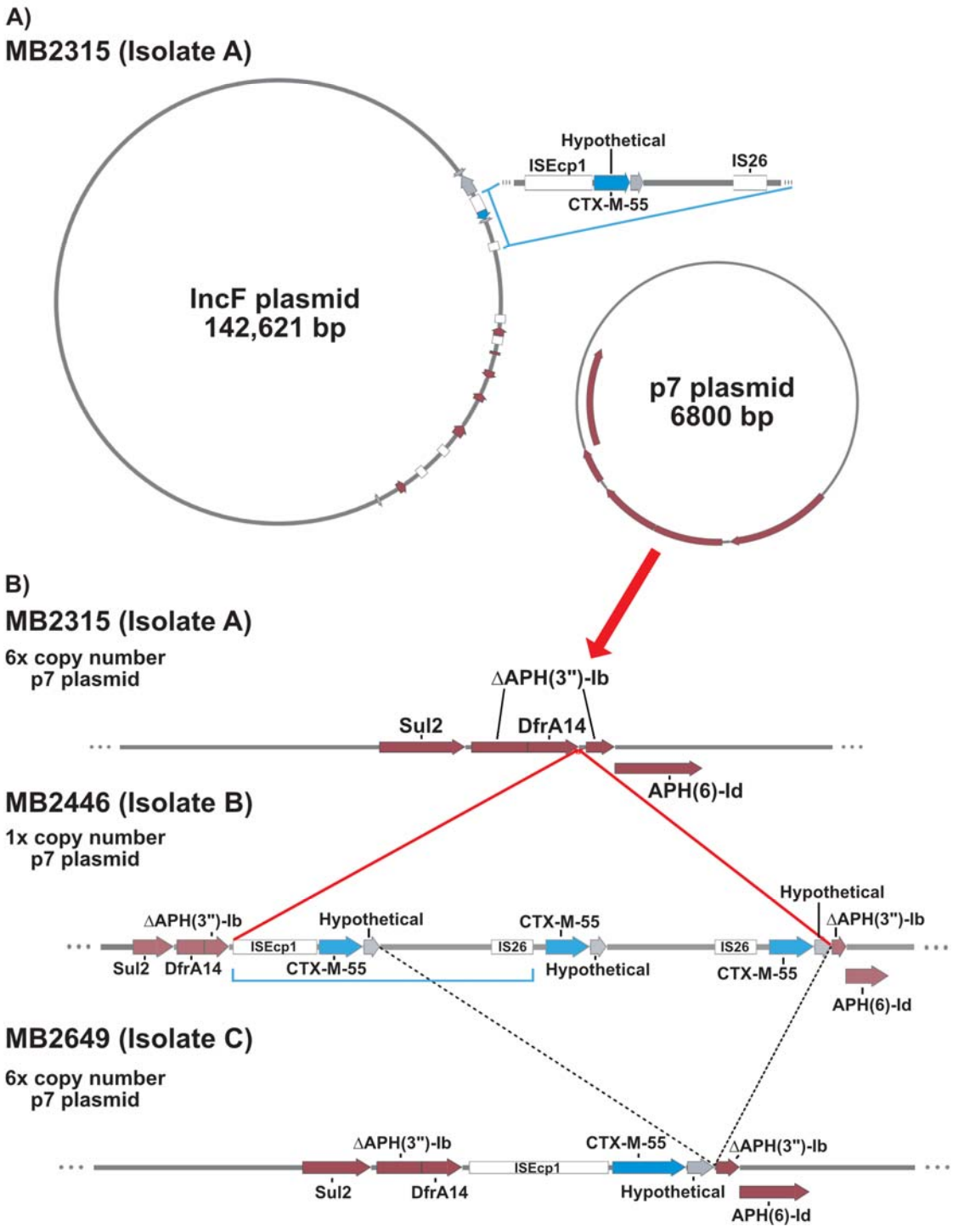

**Fig. 6. Characterization of *bla*$_{\text{CTX-M-55}}$ amplification within patient 10 serial isolates. (A)** Genomic structures of the IncF and p7 plasmids found in isolate MB2315. The blue bracketed area indicates the original location of the IS*Ecp1*-*bla*$_{\text{CTX-M-55}}$-IS*26* MB2315TU on the IncF plasmid upstream of a larger heterogeneous resistance gene island. *bla*$_{\text{CTX-M-55}}$ ORF is indicated in blue. The thick red line from panel A to B indicates that the first linear strand in panel B is the p7 plasmid with AMR determinants (maroon) annotated. **(B)** Shows the progressive change in p7 from each serial isolate noting the insertion of MB2315TU (MB2446) with subsequent drop of two copies of the TU (MB2649). Blue bracket in MB2446 is equivalent to blue bracketed region in **(A)**. Red lines indicate point of insertion of MB2315TU into p7 for MB2446 whereas dotted line between MB2446 and MB2649 p7 plasmid indicate where the TU array region was dropped.

## Detection of β-lactamase gene amplification and porin disruption by AMR elements in other *Enterobacteriaceae* strains

We identified two non-CP-CRE strains, MB101 (*K. pneumoniae*) and MB746A (*E. coli*) in a previous study examining the role of short-read whole genome sequencing (WGS) in predicting β-lactam resistance (*30*). Our short-read analysis indicated both strains had increased mapping depth of $bla_{\text{OXA-1}}$ as well as disruption of major porin genes with MB101 having increased mapping depth of $bla_{\text{CTX-M-15}}$ as well (Table 1) (*30*). Thus, we performed ONT sequencing on the two isolates to determine whether the mechanisms of gene amplification and porin disruption were similar to those observed in our serial isolates. Both isolates contain a similar IS6-mediated TU carrying $bla_{\text{OXA-1}}$ relative to the previously characterized MB1860TU (Fig. S4; Fig. S5).

Similar to strain MB1860, increased mapping depth was present in strain MB101 surrounding *aac-(6')-Ib'*, $bla_{\text{OXA-1}}$, Δ*catB3*, *aac(3')-IIc*, and *tmrB* (~11-fold). We were able to identify a single ONT read that had 9X TUs containing the aforementioned AMR genes on the MB101 chromosome. The TU repeat structure from MB101 had 100% coverage; 99.9% ID with MB1860TU found in serial isolates from patients 4 and 11 (Fig. S5A). We were unable to determine the genetic context of the 3' flanking end of the insertion due to the size of the TU and lack of an index reference genome resulting in an incomplete MB101 chromosome structure. The MB101 short-read analysis also indicated that there was higher coverage depth of $bla_{\text{CTX-M-15}}$. Similar to strain MB1860, in strain MB101 the key porin-encoding gene *ompK36* was interrupted by a unique 5.4 kb TU that carries $bla_{\text{CTX-M-15}}$ flanked by ISEcp1 and a truncated Tn2 transposase, designated as MB101TU (Fig. S4B). MB101TU is also located on an IncFIB(K)_1_Kpn3 plasmid where it has inserted within a full length Tn2 transposon (Fig. S4C). The presence of MB101TU on a plasmid inserted within a full-length Tn2 transposon, as well as the fact that a segment of the Tn2 transposon is found on the chromosomal insertion of *ompK36*, suggests a plasmid

origin for MB101TU. We also noted at least three additional insertions of *bla*$_{\text{CTX-M-15}}$ on the incomplete MB101 chromosome.

The mapping pattern for MB746A was quite similar to that of the serial isolates of patient 4 and patient 11 with increased mapping depth (~9X) of the *bla*$_{\text{OXA-1}}$ IS6-mediated TU. However, this TU has also a tetracycline resistance operon and macrolide resistance operon inserted within a similar TU structure as MB1860TU (Fig. S5A). Interestingly, we also saw a small IS26-*aac(3)-IIa-tmrB*-IS6 2X repeat (blue brackets on Fig. S5B), which may indicate a similar replicative mechanism to how the full MB1860TU and MB1860TU-like structures replicate. Taken together, these findings indicate that the gene amplification and porin inactivation mechanisms detected in our serial isolates are also present in other non-CP-CRE strains.

## Overexpression of *bla*$_{\text{OXA-1}}$, but not *bla*$_{\text{CTX-M-15}}$, increases piperacillin-tazobactam minimum inhibitory concentration

Of the 28 strains in our cohort, 16 were piperacillin-tazobactam (TZP) resistant even though only a single isolate contained a gene encoding an enzyme predicted to hydrolyze TZP (*bla*$_{\text{OXA-181}}$). In light of the recent report of *bla*$_{\text{TEM-1}}$ gene amplification leading to TZP resistance (*23*), we assessed the relationship between increased read mapping to β-lactamase encoding genes and TZP resistance. Indeed, nearly all strains with unexplained TZP resistance evidenced augmented depth of read mapping to β-lactamase encoding genes, typically for *bla*$_{\text{OXA-1}}$ (Table 1). Conversely, no TZP susceptible strain had such increased mapping depth. To directly evaluate the contribution of OXA-1 to β-lactam resistance, we cloned *bla*$_{\text{OXA-1}}$ into an arabinose inducible expression system and assessed the effect of *bla*$_{\text{OXA-1}}$ expression on ertapenem (ERT) and TZP resistance in the clean genetic background of DH5α *E. coli*, which is intrinsically sensitive to these antibiotics. Inducing *bla*$_{\text{OXA-1}}$ expression increased TZP MIC 6.8-fold relative to uninduced cells (Fig. 7B) but did not alter the ERT MIC (Fig. 7A). We observed a similar increase in TZP, but not ERT, MIC following overexpression of *bla*$_{\text{SHV-1}}$ (Fig. 7B). The lack of effect on

ERT is consistent with a previous laboratory study in which β-lactamase encoding gene amplification only increased carbapenem MIC when porins were also inactivated (*18*). Given that both $bla_{\text{OXA-1}}$ and $bla_{\text{CTX-M-15}}$ were amplified in the TZP resistant strain MB101 (Table 1), we sought to determine whether high level production of CTX-M-15 might contribute to TZP resistance. We observe no increase in ERT or TZP MIC following $bla_{\text{CTX-M-15}}$ overexpression, although an increase in ceftriaxone MIC was observed consistent with the known activity of CTX-M-15 against this antibiotic (Fig. 7C) (*33*). Together with previous data (*23*), we conclude that overexpression of a variety of narrow spectrum β-lactamase-encoding genes can drive TZP resistance.

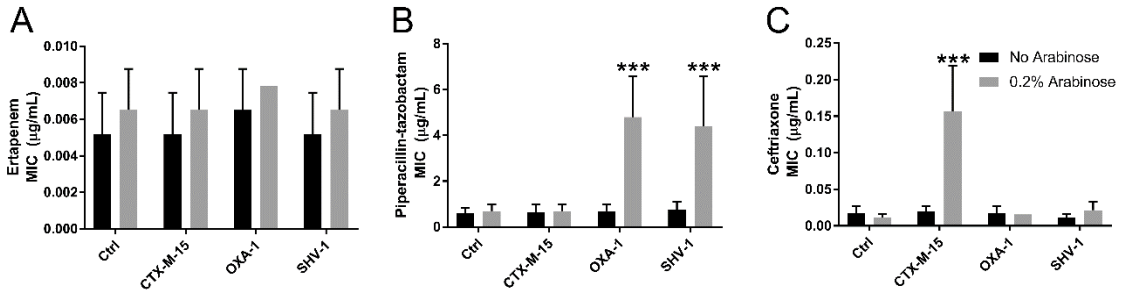


**Figure 7. *Bla*$_{\text{OXA-1}}$ and *bla*$_{\text{SHV-1}}$ expression contribute to TZP resistance.** DH5a E. coli carrying pBAD33 empty vector (Ctrl) or arabinose-inducible *bla*$_{\text{CTX-M-15}}$, *bla*$_{\text{OXA-1}}$, or *bla*$_{\text{SHV-1}}$ were exposed to ertapenem (A), piperacillin-tazobactam (B), or ceftriaxone (C) in a broth microdilution assay. Mean and standard deviation of MICs observed from at least three experiments are reported. Statistics reported as results of ANOVA with Dunnett's test of multiple comparisons against uninduced controls. *P*-value of <0.0001 shown as ***.

## Discussion

*Enterobacteriaceae* resistance to broad-spectrum β-lactams are among the most pressing AMR threats (*34*). There has been significant progress in elucidating the role of specific enzymes driving such resistance, such as carbapenemases and ESBLs (*35*). However, the underlying mechanisms of commonly observed non-CP-CRE as well as resistance to such widely used antibiotics as TZP remain poorly understood (*8, 30*). Therefore, we used serial clinical isolates to resolve their genomes using both short- and long-read technologies which in turn facilitated demonstration that non-CP-CRE emerges from ESBL-E through a combination of IS mediated β-lactamase TU translocation, subsequent β-lactamase gene amplification, and porin inactivation within our cohort. Moreover, we discovered that increased copy number of the gene encoding the class D narrow spectrum β-lactamase OXA-1 was strongly associated with TZP resistance in clinical isolates and that augmented $bla_{\text{OXA-1}}$ expression increased TZP MIC under laboratory conditions. Taken together, these data markedly extend understanding of the mechanisms of progressive β-lactam resistance amongst *Enterobacteriaceae*.

Among the key findings of this study was that development of carbapenem resistance from an ESBL-E background rarely occurred due to acquisition of new genetic material but was rather due to adaptive mechanisms including mutations in porin genes and AMR encoding gene amplification. The single instance of carbapenemase acquisition in our study was due to replacement of an ESBL-E isolate with a completely new strain (patient 7). Our clinical findings regarding the role of porin loss and β-lactamase gene amplification leading to development of CRE generally mirrors laboratory-based analyses with a few key differences (*10-12, 18, 20, 36*). Laboratory studies that generated CRE strains through serial passaging have consistently found that OmpC and OmpF porin production is reduced in carbapenem resistant isolates, but mechanisms have generally involved alterations in the porin regulatory protein OmpR or in OmpR binding sites (*18, 20*). Similarly, a recent study of a single patient with recurrent *E. coli* infection identified a single amino change in OmpR as leading to loss of OmpC and OmpF expression with development of ertapenem resistance (*15*). Conversely, we observed direct inactivation

of OmpC and OmpF via TU translocation or via insertions/deletions that resulted in frame-shifts whereas no alterations in OmpR were identified in our cohort. Although there have been reports of a wide variety of insertion sequences interrupting porin genes (*37, 38*), we are not aware of previous identification of porin interruption due to the translocation of TUs carrying AMR determinants. Given the length of the TUs as well as the fact that they have the ability to amplify and create TU arrays once inserted into the porin encoding genes, it is unlikely that targeted PCR based strategies or commonly used short-read approaches alone would have been able to identify the full extent of the TUs observed in our study. Thus, performing long read sequencing on larger cohorts of porin inactivated *Enterobacteriaceae* should help reveal whether AMR-carrying TUs mediating the disruption of porin genes occur widely but have not been previously identified due to the long and repetitive nature of the involved DNA structures.

The finding that $bla_{\text{OXA-1}}$ amplification was consistently associated with progressive development of β-lactam resistance was somewhat surprising given that this enzyme is typically considered a narrow spectrum β-lactamase, although investigations have been limited particularly in regards to the activity of OXA-1-harboring organisms conferring TZP resistance (*39*). Several studies have found that cloning of $bla_{\text{OXA-1}}$ onto a plasmid in *E. coli* resulted in TZP MICs that were in the resistant range (*40, 41*), yet there also have been consistent findings that *Enterobacteriaceae* strains containing $bla_{\text{OXA-1}}$ can have TZP MICs ranging from fully susceptible to highly resistant (*30, 42, 43*). Indeed, in the recent MERINO trial that studied treatment of ESBL-E strains susceptible to TZP, 67.6% of strains contained $bla_{\text{OXA-1}}$ or variants indicating that the presence of the $bla_{\text{OXA-1}}$ gene alone is not sufficient to confer TZP resistance (*44*). Using a plasmid capable of differentially expressing $bla_{\text{OXA-1}}$, we herein begin to resolve the somewhat enigmatic relationship between $bla_{\text{OXA-1}}$ and TZP susceptibility by showing a linear relationship between $bla_{\text{OXA-1}}$ expression and TZP MICs. Our data, combined with previously published analyses (*23*), indicate an effect between *bla* gene quantity and TZP resistance. The genetic arrangement of *aac-(6')-Ib'*, $bla_{\text{OXA-1}}$, Δ*catB3* in association with IS26 elements that were amplified in our strains is being increasingly recognized with Livermore et al. recently finding co-presence of *aac-(6')-Ib'* and $bla_{\text{OXA-1}}$ in

147/149 *bla*$_{OXA-1}$ containing *E. coli* strains (*32*, *42*). Thus, augmented *bla*$_{OXA-1}$ expression may be quite common in *E. coli* and perhaps other *Enterobacteriaceae* given our finding of a highly similar *bla*$_{OXA-1}$ containing TU in a *K. pneumoniae* strain (MB101).

Augmented expression of β-lactamase encoding genes has long been recognized in *Enterobacteriaceae* (*19*, *45*), but the long reads afforded by ONT sequencing allowed for direct visualization of an IS*26* mediated mechanism. A report of a *K. pneumoniae* outbreak in 2012 identified a 220 kbp plasmid named pUUH239.2 containing IS26 elements, *bla*$_{CTX-M-15}$, *bla*$_{TEM-1}$, and *bla*$_{OXA-1}$ that had previously been isolated from ST131 *E. coli* (*32*). The authors reported a suspected gene "triplication" involving IS*26* elements in pUUH239.2 based on high-density short read mapping but did not specify the location. Moreover, when a strain containing pUUH2392.2 was passaged in the presence of carbapenems, there were increased copy numbers of *bla* genes, particularly *bla*$_{OXA-1}$ (*18*). Similarly, the identification of the extensive co-presence of *bla*$_{OXA-1}$ and *aac-(6')-Ib'* noted that these genes were commonly present in the vicinity of IS*26* elements but that the repetitive nature of the region made assembly via short read data impossible (*42*). Recent studies have shed insight into the potential mechanisms by which IS*26*-mediated translocatable units could create resistance gene arrays through both RecA-independent replication and RecA-dependent conservative (*i.e.* homologous recombination) mechanisms (*46-48*). Based on these previous studies as well as our own serial isolate data from patient 4, we hypothesize that the initial incorporation of the IS*26*-mediated TU as well as other translocations into the flanking regions of the chromosome occurred via a RecA-independent replication mechanism; gene amplification then occurred via homologous recombination. The high rates of IS*26* elements in association with various *bla* genes (*46*) means that a diverse array of *Enterobacteriaceae* strains may have the capacity to develop progressive β-lactam resistance independently of the acquisition of exogenous β-lactamase encoding elements.

Nevertheless, it is important to note that IS*26* mediated amplification of a TU was not the only mechanism of *Enterobacteriaceae* gene amplification present in our cohort. In patient 10, a complex series of events occurred which eventually resulted in IS*Ecp1* in association with $bla_{\text{CTX-M-55}}$ being present on a high copy number plasmid (Fig. 6). This mechanism of gene amplification is similar to that in a recent study examining development of carbapenem resistance in association with increased copy number of an IncI plasmid encoding CMY-2 in an *E. coli* strain due to a mutation in the *inc* gene that controls plasmid copy number (*20*). Similarly, MB1860TU containing $bla_{\text{OXA-1}}$ as well as $bla_{\textit{CTX-M-15}}$ were present on both the chromosome and an IncF plasmid in patient 11 possibly indicating a mechanism by which this TU could be transferred intercellularly.

Despite the varied mechanisms present in our cohort, the *bla* gene amplification events could be readily identified using short-read data (Table 1) indicating the potential importance of incorporating read mapping depth into WGS based genotype-AMR phenotype relationships (*30*). Moreover, these findings provide a mechanism by which widely clinically used PCR based methodologies of assessing AMR, which cannot identify gene amplification events, may incorrectly predict strain AMR phenotypes (*49*).

In conclusion, we have used a combination of serial clinical isolates subjected to complementary WGS approaches to identify that a combination of porin inactivation and IS-mediated amplification of β-lactamase encoding genes underlies the emergence of non-CP-CRE from ESBL in *Enterobacteriaceae.* We predict that more widespread application of long-read sequencing technologies will facilitate appreciation of the mechanisms and impact of TU-mediated translocations, porin disruptions, and gene amplifications on a diverse array of AMR pathogens.

# Materials and Methods

## Stain identification and clinical data analysis

We performed a retrospective cohort review of patients with ESBL-E bacteremia between January 2015 and July 2016 at The University of Texas MD Anderson Cancer Center in Houston, Texas. All patients with one or more episodes of ESBL-E bacteremia and who were 18 years old or greater were eligible for inclusion. Clinical and demographic characteristics were manually extracted from the electronic medical record and recorded using REDCap software (Vanderbilt University, Nashville, TN) (*50*). A waiver of informed consent to collect clinical data and analyze the isolates was provided by the MDACC IRB (PA15-0799). Antibiotic susceptibility testing was performed per routine clinical laboratory practice using an automated system (Vitek2 [bioMérieux, Marcy L'Étoile, France]) with additional testing performed as needed using individual antibiotic gradient strips (Etest [bioMérieux]). ESBL production was assessed per routine laboratory practice on *E. coli*, *K. pneumonia*, and *K. oxytoca* isolates that were resistant to one or more oxyimino-cephalosporins (e.g. cefotaxime, ceftriaxone, or ceftazidime) using either the ESBL Etest (bioMérieux) or the Rapid ESBL Screen kit (Rosco, Taastrup, Denmark). Carbapenemase production was evaluated in the clinical lab on any Enterobacteriaceae isolate resistant to one more of the carbapenems using the Neo-Rapid CARB kit (Rosco) according to manufacturer's instructions. Recurrent bacteremia was defined as identification of organism of the same species in blood culture at any point during the follow-up period following at least one negative blood culture and completion of an antibiotic treatment regimen. Carbapenem resistance (CR) was defined as resistance to either ertapenem or meropenem using CLSI criteria (*51*).

Two additional strains, MB746A and MB101, are the sole carbapenem resistant, carbapenemase negative *E. coli* and *K. pneumoniae* strains respectively, present in a previously published study examining the role of whole genome sequencing (WGS) in predicting β-lactam resistance (*30*).

## Illumina sequencing data analysis

Blood culture isolates are routinely saved at our institution, and all available paired isolates (i.e., isolates from recurrent bacteremia patients) initially underwent whole genome sequencing (WGS) via Illumina HiSeq as described previously (*30*). The paired-end short-reads were assessed using the FastQC toolkit (Babraham Institute); adaptors as well as low quality reads were trimmed using Trimmomatic v0.33 (*52*). Genome assembly was performed using SPAdes v3.9.1 (*53*). Depth of short read mapping to individual AMR encoding genes was quantitated relative to the average read mapping depth for the single-copy ribosome protein encoding genes rplM, rplN, rpsM, rpsS, and rpsH.

In order to determine clonality of isolates, we used a phylogenetic analysis approach along with *in silico* MLST. The pan-genome pipeline tool Roary-v3.12.0 was used to perform a core genome alignment of the SPAdes assembled genomes using the probabilistic alignment program PRANK (*54, 55*). A core genome SNP matrix was generated with this data using an in-house custom Python script, which was subsequently used to build a maximum likelihood (ML) phylogenetic tree using RAxML-v8.2.12 (*56*). Multi-locus sequencing typing (MLST) was performed *in silico* using mlst-v2.15.1 (Seemann, T mlst Github: https://github.com/tseemann/mlst; (*57*)) followed by the analysis of nested population structures within the ML phylogenetic tree using hierBAPS-v1.0.1 (*58, 59*).

## Oxford Nanopore Technology (ONT) sequencing analysis

Serial, clonal isolates that demonstrated progressive β-lactam resistance as well as end-stage strains MB746A and MB10 that had previously undergone Illumina sequencing (*30*), underwent Oxford Nanopore Technology (ONT) sequencing. Library preps were completed using the SQK-RBK004 rapid barcoding kit and run on ONT MinION R9.4.1 flow cells using the ONT GridION X5 (Oxford, UK).

ONT fast5 data was generated using ONT MinKNOW software (2.2 v18.08.2) with subsequent base-calling using albacore-2.3.1. *De* novo assemblies were performed using Canu-v1.8 (*60*). Assemblies underwent one round of short-read polishing using the HiSeq Illumina data with Racon-v.1.3.1 (*61*). The assembled, polished contigs were then manually inspected along with their *de novo* assembly graphs using the dotplot software package Gepard-v1.40 (*62*) and Bandage-v0.8.1(*63*) respectively. The python script simple-circularise.py (Kitson, E Simple-Circularise Github: https://github.com/Kzra/Simple-Circularise) was used to close complete circular structures, while Prokka-v1.13.3 (*64*) was used to find the *dnaA* gene for standardization of the chromosomal three prime start region. Plasmids were standardized, when possible with replication initiator protein genes identified with abricate-v0.8.10 (Seemann, T abricate Github: https://github.com/tseemann/abricate) using the PlasmidFinder database (updated 2018/11/24) (*65*). Contigs were then concatenated back into a multi-fasta file and underwent one round of long-read polishing with Nanopolish-v0.11.0 (Simpson, J nanopolish Github: https://github.com/jts/nanopolish) followed by multiple rounds of racon polishing (*61*). The number of rounds of Racon polishing necessary were determined by mapping short-reads back onto the *de novo* assemblies and looking for the reduction of erroneous SNP calls using Snippy-v4.3.6 (Seemann, T snippy Github: https://github.com/tseemann/snippy). Once SNP calls were reduced to zero or plateaued to a minimum, we deemed this a consensus assembly. In particular cases where the assemblies were highly fragmented using solely Canu, these contigs were used as scaffolds along with both the short and long reads to create a hybrid assembly using the Unicycler-v0.4.7 wrapper with the –existing_long_read_assembly parameter (*66*). Final polished assemblies in both instances were then re-annotated using Prokka-v1.13.3 (*64*) wherein they underwent further analysis described in the following sections [41].

## Identification of AMR elements and genetic variance among serial isolates

Presence of AMR elements was assessed using the Illumina HiSeq data using a previously published AMR detection pipeline (*30*). Variation in genetic content between the serial isolates was determined by

mapping short-read Illumina HiSeq data to the closed genome of the original isolate using Geneious-v11.0. All detected variations were confirmed via manual inspection of the mapping data as well as inspection of the complete *de novo* genome assemblies generated via ONT sequencing.

Identification of AMR determinants and mobile genetic elements (MGEs) of interest located on the long-read data were parsed out using a multifaceted process. First, assembled consensus genomes as well as individual contigs were parsed with ABRicate (Seemann, T ABRicate Github: https://github.com/tseemann/abricate) using the Comprehensive Antibiotic Resistance Database (CARD)(*67*) and PlasmidFinder(*65*) to search for AMR determinants and MGEs respectively. Additionally, annotated Prokka gff files were used to characterize other ORFs of interests as well as confirm the results found with ABRicate. Lastly, CARD, PlasmidFinder, and BLAST webtools were heavily utilized during manual inspection of the assemblies using SnapGene v4.3 (SnapGene software [from GSL Biotech; available at snapgene.com]) to ensure correct context of annotated features.

In cases where assemblies were not completely resolved due to putative large repeat regions that could not be fully captured on ONT long reads, we used a newly developed tool SVAnts-v0.1 (Hanson, B SVAnts Github:https://github.com/EpiBlake/SVAnts) to investigate subsets of ONT long reads. Briefly, this tool enabled us to find translocatable units (TUs) of interest captured fully or partially on individual reads as well as identify the regions in which the TU was inserted within a well assembled and annotated reference genome.

## β-lactamase encoding gene and gene transcript level analysis

For both DNA and RNA quantitative reverse transcription PCR (qRT-PCR), indicated strains were grown in triplicate on two separate days (six biologic replicates) to mid-exponential phase ($OD_{600}$ ~ 0.5) in Luria-Bertani (LB) broth (ThermoFisher) at 37º C shaking at 220 rpm. DNA isolation was performed using the DNEasy kit (Qiagen) and qRT-PCR was performed using TaqMan reagents on the StepOne

Plus Real Time PCR. The DNA levels of *bla*$_{OXA-1}$ and *bla*$_{CTX-M}$ were determined relative to the *rpsL* control gene using the ΔCt method (*18*).

For RNA analysis, cells were mixed 1:2 with RNAProtect (Qiagen) and harvested via centrifugation. RNA was isolated from cell pellets using the RNEasy kit (Qiagen) and converted to cDNA using the High Capacity cDNA Reverse Transcription kKit (Applied Biosystems). Relative transcript levels of the β-lactamase encoding genes (*bla*$_{OXA-1}$ and *bla*$_{CTX-M}$) were assayed using TaqMan reagents on the StepOne Plus Real Time PCR machine (Applied Biosystems). The transcript level of *bla*$_{OXA-1}$ and *bla*$_{CTX-M}$ were determined relative to the endogenous control gene *rpsL* (*68*) using the ΔCt method. QRT-PCR Primers and Probes are provided in Table S2.

## β-lactamase cloning and expression

The open reading frames of β-lactamases were amplified from genomic DNA of the *K. pneumoniae* strain MB101 using Q5 polymerase and the primers listed in Table S2. Cloned ORFs were inserted into the arabinose inducible vector pBAD33 by Gibson assembly (*69*) of purified products. pBAD33*bla*$_{CTX-M-15}$ and pBAD33*bla*$_{OXA-1}$ were transformed into DH5α *E. coli* and were maintained with 50μg/mL chloramphenicol in cation adjusted Mueller Hinton (MHII) media. Minimum inhibitor concentration (MIC) assays were performed with ceftriaxone (Sandoz GmbH), ertapenem (Merck), or piperacillin-tazobactam (Fresenius Kabi USA) as follows. DH5α strains carrying pBAD33*bla*$_{CTX-M-15}$, pBAD33*bla*$_{OXA-1}$, or control vector were grown for 18 hours at 220 rpm at 37$^{o}$C in MHII with 50μg/mL chloramphenicol. These cultures were diluted to approximately 5x10$^{5}$ CFU/mL in MHII with 0.2% L-Arabinose or vehicle control, without chloramphenicol. Each strain was exposed to serial dilutions of the above drugs in microtiter plates sealed with gas-permeable membranes (Midsci). Microtiter plates were incubated for 18 hours at 220rpm at 37$^{o}$C, followed by OD$_{600}$ measurement in a Biotek Synergy HT plate reader. The lowest tested antibiotic concentration yielding OD$_{600}$ measurement of 0.06 or less in at least two of three replicate wells was considered to be the MIC.

## Statistical analyses

Bivariate comparisons between patients with recurrent bacteremia and patients with a single bacteremia episode were made with the Wilcoxon Rank-sum test and Fisher's exact test as appropriate based on covariate distributions. Comparisons of DNA and RNA levels among strains was performed using the Kruskall-Wallis test (when more than two strains were analyzed) or the Wilcoxon Rank-sum test (when two strains were analyzed). MIC comparisons were performed using ANOVA with Dunnett's test of multiple comparisons. Statistical significance was assigned as a two-sided $P$ value $< 0.05$.

**Acknowledgments:** We thank the personnel of the clinical microbiology laboratory at MD Anderson Cancer Center for assistance with collecting isolates.

**Funding**: Financial support for this study was provided by the Shelby Foundation (R. Lee Clark Fellow Award to SAS). Sequencing was performed at the MDACC DNA sequencing facility which is supported by the National Cancer Institute [grant number P30-CA016672 via the Bioinformatics Shared Resource]. JK is supported by the Cancer Prevention and Research Institute of Texas (RP150596). Other support provided by the UT Southwestern DocStars award (DEG, JK). JGP is supported by the NIAID (1K01AI143881-01). CAA is supported by NIH/NIAID grants K24AI121296 (CAA), R01AI134637 (CAA), R21AI143229 (CAA) and UTHealth Presidential Collaborative Award

**Author contributions:**

WCS – developed the database, generated and analyzed the data, wrote the paper

SLA – designed the study, collected and analyzed the data, wrote the paper

RP – designed the study, performed the experiments, analyzed the data

JK – performed the experiments, analyzed the data

MB – performed the experiments, wrote the paper

XL – performed phylogenomic analyses

AK – performed phylogenomic analyses, wrote the paper

JGP – designed the study, analyzed the isolates, wrote the paper

PS – collected and curated the isolates

CAA – designed the study, analyzed the data, wrote the paper

DEG- analyzed the data, wrote the paper

BMH – wrote scripts to analyze the data, analyzed the data, wrote the paper

SAS – designed the study, analyzed the data, wrote the paper

**Competing interests**: None

**Data and materials availability**: The sequences reported in this paper have been deposited in the National Center for Biotechnology BioProject database (accession number pending)

# References and Notes:


1. A. Chioro, A. M. Coll-Seck, B. Hoie, N. Moeloek, A. Motsoaledi, R. Rajatanavin, M. Touraine, Antimicrobial resistance: a priority for global health action. *Bull World Health Organ* **93**, 439 (2015).
2. C. f. D. C. a. Prevention.
3. H. W. Boucher, G. H. Talbot, J. S. Bradley, J. E. Edwards, D. Gilbert, L. B. Rice, M. Scheld, B. Spellberg, J. Bartlett, Bad bugs, no drugs: no ESKAPE! An update from the Infectious Diseases Society of America. *Clin Infect Dis* **48**, 1-12 (2009).
4. A. Y. Guh, B. M. Limbago, A. J. Kallen, Epidemiology and prevention of carbapenem-resistant Enterobacteriaceae in the United States. *Expert Rev Anti Infect Ther* **12**, 565-580 (2014).
5. N. Gupta, B. M. Limbago, J. B. Patel, A. J. Kallen, Carbapenem-resistant Enterobacteriaceae: epidemiology and prevention. *Clin Infect Dis* **53**, 60-67 (2011).
6. A. Iovleva, Y. Doi, Carbapenem-Resistant Enterobacteriaceae. *Clin Lab Med* **37**, 303-315 (2017).
7. L. K. Logan, R. A. Weinstein, The Epidemiology of Carbapenem-Resistant Enterobacteriaceae: The Impact and Evolution of a Global Menace. *J Infect Dis* **215**, S28-S36 (2017).
8. A. Y. Guh, S. N. Bulens, Y. Mu, J. T. Jacob, J. Reno, J. Scott, L. E. Wilson, E. Vaeth, R. Lynfield, K. M. Shaw, P. M. Vagnone, W. M. Bamberg, S. J. Janelle, G. Dumyati, C. Concannon, Z. Beldavs, M. Cunningham, P. M. Cassidy, E. C. Phipps, N. Kenslow, T. Travis, D. Lonsway, J. K. Rasheed, B. M. Limbago, A. J. Kallen, Epidemiology of Carbapenem-Resistant Enterobacteriaceae in 7 US Communities, 2012-2013. *JAMA* **314**, 1479-1487 (2015).
9. G. A. Jacoby, D. M. Mills, N. Chow, Role of beta-lactamases and porins in resistance to ertapenem and other beta-lactams in Klebsiella pneumoniae. *Antimicrob Agents Chemother* **48**, 3203-3206 (2004).
10. H. Mammeri, P. Nordmann, A. Berkani, F. Eb, Contribution of extended-spectrum AmpC (ESAC) beta-lactamases to carbapenem resistance in Escherichia coli. *FEMS Microbiol Lett* **282**, 238-240 (2008).
11. Y. K. Tsai, C. H. Liou, C. P. Fung, J. C. Lin, L. K. Siu, Single or in combination antimicrobial resistance mechanisms of Klebsiella pneumoniae contribute to varied susceptibility to different carbapenems. *PLoS One* **8**, e79640 (2013).
12. T. Tangden, M. Adler, O. Cars, L. Sandegren, E. Lowdin, Frequent emergence of porin-deficient subpopulations with reduced carbapenem susceptibility in ESBL-producing Escherichia coli during exposure to ertapenem in an in vitro pharmacokinetic model. *J Antimicrob Chemother* **68**, 1319-1326 (2013).
13. P. L. Ho, Y. Y. Cheung, Y. Wang, W. U. Lo, E. L. Lai, K. H. Chow, V. C. Cheng, Characterization of carbapenem-resistant Escherichia coli and Klebsiella pneumoniae from a healthcare region in Hong Kong. *Eur J Clin Microbiol Infect Dis* **35**, 379-385 (2016).
14. A. Agyekum, A. Fajardo-Lubian, X. Ai, A. N. Ginn, Z. Zong, X. Guo, J. Turnidge, S. R. Partridge, J. R. Iredell, Predictability of Phenotype in Relation to Common beta-Lactam Resistance Mechanisms in Escherichia coli and Klebsiella pneumoniae. *J Clin Microbiol* **54**, 1243-1250 (2016).
15. H. Dupont, P. Choinier, D. Roche, S. Adiba, M. Sookdeb, C. Branger, E. Denamur, H. Mammeri, Structural Alteration of OmpR as a Source of Ertapenem Resistance in a CTX-M-15-Producing Escherichia coli O25b:H4 Sequence Type 131 Clinical Isolate. *Antimicrob Agents Ch* **61**, (2017).
16. Z. Hamzaoui, A. Ocampo-Sosa, M. F. Martinez, S. Landolsi, S. Ferjani, E. Maamar, M. Saidani, A. Slim, L. Martinez-Martinez, I. B. Boubaker, Role of association of OmpK35 and OmpK36 alteration and blaESBL and/or blaAmpC in conferring carbapenem resistance among non-

producing carbapenemase-Klebsiella pneumoniae. *International journal of antimicrobial agents*, (2018).

17. P. A. Bradford, C. Urban, N. Mariano, S. J. Projan, J. J. Rahal, K. Bush, Imipenem resistance in Klebsiella pneumoniae is associated with the combination of ACT-1, a plasmid-mediated AmpC beta-lactamase, and the foss of an outer membrane protein. *Antimicrob Agents Chemother* **41**, 563-569 (1997).
18. M. Adler, M. Anjum, D. I. Andersson, L. Sandegren, Influence of acquired beta-lactamases on the evolution of spontaneous carbapenem resistance in Escherichia coli. *J Antimicrob Chemother* **68**, 51-59 (2013).
19. L. Sandegren, D. I. Andersson, Bacterial gene amplification: implications for the evolution of antibiotic resistance. *Nat Rev Microbiol* **7**, 578-588 (2009).
20. R. van Boxtel, A. A. Wattel, J. Arenas, W. H. Goessens, J. Tommassen, Acquisition of Carbapenem Resistance by Plasmid-Encoded-AmpC-Expressing Escherichia coli. *Antimicrob Agents Chemother* **61**, (2017).
21. W. H. Goessens, A. K. van der Bij, R. van Boxtel, J. D. Pitout, P. van Ulsen, D. C. Melles, J. Tommassen, Antibiotic trapping by plasmid-encoded CMY-2 beta-lactamase combined with reduced outer membrane permeability as a mechanism of carbapenem resistance in Escherichia coli. *Antimicrob Agents Chemother* **57**, 3941-3949 (2013).
22. A. Beceiro, S. Maharjan, T. Gaulton, M. Doumith, N. C. Soares, H. Dhanji, M. Warner, M. Doyle, M. Hickey, G. Downie, G. Bou, D. M. Livermore, N. Woodford, False extended-spectrum {beta}-lactamase phenotype in clinical isolates of Escherichia coli associated with increased expression of OXA-1 or TEM-1 penicillinases and loss of porins. *J Antimicrob Chemother* **66**, 2006-2010 (2011).
23. L. M. Schechter, D. P. Creely, C. D. Garner, D. Shortridge, H. Nguyen, L. Chen, B. M. Hanson, E. Sodergren, G. M. Weinstock, W. M. Dunne, Jr., A. van Belkum, S. R. Leopold, Extensive Gene Amplification as a Mechanism for Piperacillin-Tazobactam Resistance in Escherichia coli. *MBio* **9**, (2018).
24. L. Poirel, C. Heritier, C. Spicq, P. Nordmann, In vivo acquisition of high-level resistance to imipenem in Escherichia coli. *J Clin Microbiol* **42**, 3831-3833 (2004).
25. J. Oteo, A. Delgado-Iribarren, D. Vega, V. Bautista, M. C. Rodriguez, M. Velasco, J. M. Saavedra, M. Perez-Vazquez, S. Garcia-Cobos, L. Martinez-Martinez, J. Campos, Emergence of imipenem resistance in clinical Escherichia coli during therapy. *Int J Antimicrob Agents* **32**, 534-537 (2008).
26. J. H. Chia, L. K. Siu, L. H. Su, H. S. Lin, A. J. Kuo, M. H. Lee, T. L. Wu, Emergence of carbapenem-resistant Escherichia coli in Taiwan: resistance due to combined CMY-2 production and porin deficiency. *J Chemother* **21**, 621-626 (2009).
27. C. Y. Kao, J. W. Chen, T. L. Liu, J. J. Yan, J. J. Wu, Comparative Genomics of Escherichia coli Sequence Type 219 Clones From the Same Patient: Evolution of the IncI1 blaCMY-Carrying Plasmid in Vivo. *Front Microbiol* **9**, 1518 (2018).
28. S. Nuramrum, A. Chanawong, K. Lunha, A. Lulitanond, A. Sangka, C. Wilailuckana, S. Angkititrakul, N. Charoensri, L. Wonglakorn, P. Chaimanee, P. Chetchotisakd, Molecular Characterization of Carbapenemase-Nonproducing Clinical Isolates of Escherichia coli (from a Thai University Hospital) with Reduced Carbapenem Susceptibility. *Jpn J Infect Dis* **70**, 628-634 (2017).
29. G. C. Cerqueira, A. M. Earl, C. M. Ernst, Y. H. Grad, J. P. Dekker, M. Feldgarden, S. B. Chapman, J. L. Reis-Cunha, T. P. Shea, S. Young, Q. Zeng, M. L. Delaney, D. Kim, E. M. Peterson, T. F. O'Brien, M. J. Ferraro, D. C. Hooper, S. S. Huang, J. E. Kirby, A. B. Onderdonk, B. W. Birren, D. T. Hung, L. A. Cosimi, J. R. Wortman, C. I. Murphy, W. P. Hanage, Multi-institute analysis of carbapenem

resistance reveals remarkable diversity, unexplained mechanisms, and limited clonal outbreaks. *Proc Natl Acad Sci U S A* **114**, 1135-1140 (2017).

30. S. A. Shelburne, J. Kim, J. M. Munita, P. Sahasrabhojane, R. K. Shields, E. G. Press, X. Li, C. A. Arias, B. Cantarel, Y. Jiang, M. S. Kim, S. L. Aitken, D. E. Greenberg, Whole-Genome Sequencing Accurately Identifies Resistance to Extended-Spectrum beta-Lactams for Major Gram-Negative Bacterial Pathogens. *Clin Infect Dis* **65**, 738-745 (2017).
31. S. R. Partridge, Z. Zong, J. R. Iredell, Recombination in IS26 and Tn2 in the evolution of multiresistance regions carrying blaCTX-M-15 on conjugative IncF plasmids from Escherichia coli. *Antimicrob Agents Chemother* **55**, 4971-4978 (2011).
32. L. Sandegren, M. Linkevicius, B. Lytsy, A. Melhus, D. I. Andersson, Transfer of an Escherichia coli ST131 multiresistance cassette has created a Klebsiella pneumoniae-specific plasmid associated with a major nosocomial outbreak. *J Antimicrob Chemother* **67**, 74-83 (2012).
33. G. O. Gutkind, J. Di Conza, P. Power, M. Radice, beta-lactamase-mediated resistance: a biochemical, epidemiological and genetic overview. *Curr Pharm Des* **19**, 164-208 (2013).
34. CDC. (2013).
35. K. Bush, Past and Present Perspectives on beta-Lactamases. *Antimicrob Agents Chemother* **62**, (2018).
36. D. Girlich, L. Poirel, P. Nordmann, CTX-M expression and selection of ertapenem resistance in Klebsiella pneumoniae and Escherichia coli. *Antimicrob Agents Chemother* **53**, 832-834 (2009).
37. A. I. Lev, E. I. Astashkin, R. Z. Shaikhutdinova, M. E. Platonov, N. N. Kartsev, N. V. Volozhantsev, O. N. Ershova, E. A. Svetoch, N. K. Fursova, Identification of IS1R and IS10R elements inserted into ompk36 porin gene of two multidrug-resistant Klebsiella pneumoniae hospital strains. *FEMS Microbiol Lett* **364**, (2017).
38. A. Mena, V. Plasencia, L. Garcia, O. Hidalgo, J. I. Ayestaran, S. Alberti, N. Borrell, J. L. Perez, A. Oliver, Characterization of a large outbreak by CTX-M-1-producing Klebsiella pneumoniae and mechanisms leading to in vivo carbapenem resistance development. *J Clin Microbiol* **44**, 2831-2837 (2006).
39. B. A. Evans, S. G. Amyes, OXA beta-lactamases. *Clin Microbiol Rev* **27**, 241-263 (2014).
40. C. Heritier, L. Poirel, D. Aubert, P. Nordmann, Genetic and functional analysis of the chromosome-encoded carbapenem-hydrolyzing oxacillinase OXA-40 of Acinetobacter baumannii. *Antimicrob Agents Chemother* **47**, 268-273 (2003).
41. C. R. Bethel, A. M. Distler, M. W. Ruszczycky, M. P. Carey, P. R. Carey, A. M. Hujer, M. Taracila, M. S. Helfand, J. M. Thomson, M. Kalp, V. E. Anderson, D. A. Leonard, K. M. Hujer, T. Abe, A. M. Venkatesan, T. S. Mansour, R. A. Bonomo, Inhibition of OXA-1 beta-lactamase by penems. *Antimicrob Agents Chemother* **52**, 3135-3143 (2008).
42. D. M. Livermore, M. Day, P. Cleary, K. L. Hopkins, M. A. Toleman, D. W. Wareham, C. Wiuff, M. Doumith, N. Woodford, OXA-1 beta-lactamase and non-susceptibility to penicillin/beta-lactamase inhibitor combinations among ESBL-producing Escherichia coli. *J Antimicrob Chemother*, (2018).
43. W. Cullmann, M. Stieglitz, Antibacterial activity of piperacillin and tazobactam against beta-lactamase-producing clinical isolates. *Chemotherapy* **36**, 356-364 (1990).
44. P. N. A. Harris, P. A. Tambyah, D. C. Lye, Y. Mo, T. H. Lee, M. Yilmaz, T. H. Alenazi, Y. Arabi, M. Falcone, M. Bassetti, E. Righi, B. A. Rogers, S. Kanj, H. Bhally, J. Iredell, M. Mendelson, T. H. Boyles, D. Looke, S. Miyakis, G. Walls, M. Al Khamis, A. Zikri, A. Crowe, P. Ingram, N. Daneman, P. Griffin, E. Athan, P. Lorenc, P. Baker, L. Roberts, S. A. Beatson, A. Y. Peleg, T. Harris-Brown, D. L. Paterson, M. T. Investigators, N. the Australasian Society for Infectious Disease Clinical Research, Effect of Piperacillin-Tazobactam vs Meropenem on 30-Day Mortality for Patients With E coli or

Klebsiella pneumoniae Bloodstream Infection and Ceftriaxone Resistance: A Randomized Clinical Trial. *JAMA* **320**, 984-994 (2018).

45. S. Normark, T. Edlund, T. Grundstrom, S. Bergstrom, H. Wolf-Watz, Escherichia coli K-12 mutants hyperproducing chromosomal beta-lactamase by gene repetitions. *J Bacteriol* **132**, 912-922 (1977).
46. C. J. Harmer, R. A. Moran, R. M. Hall, Movement of IS26-associated antibiotic resistance genes occurs via a translocatable unit that includes a single IS26 and preferentially inserts adjacent to another IS26. *MBio* **5**, e01801-01814 (2014).
47. C. J. Harmer, R. M. Hall, IS26-Mediated Precise Excision of the IS26-aphA1a Translocatable Unit. *MBio* **6**, e01866-01815 (2015).
48. C. J. Harmer, R. M. Hall, IS26-Mediated Formation of Transposons Carrying Antibiotic Resistance Genes. *mSphere* **1**, (2016).
49. S. R. Evans, A. M. Hujer, H. Jiang, K. M. Hujer, T. Hall, C. Marzan, M. R. Jacobs, R. Sampath, D. J. Ecker, C. Manca, K. Chavda, P. Zhang, H. Fernandez, L. Chen, J. R. Mediavilla, C. B. Hill, F. Perez, A. M. Caliendo, V. G. Fowler, Jr., H. F. Chambers, B. N. Kreiswirth, R. A. Bonomo, G. Antibacterial Resistance Leadership, Rapid Molecular Diagnostics, Antibiotic Treatment Decisions, and Developing Approaches to Inform Empiric Therapy: PRIMERS I and II. *Clin Infect Dis* **62**, 181-189 (2016).
50. P. A. Harris, R. Taylor, R. Thielke, J. Payne, N. Gonzalez, J. G. Conde, Research electronic data capture (REDCap)--a metadata-driven methodology and workflow process for providing translational research informatics support. *J Biomed Inform* **42**, 377-381 (2009).
51. C. a. L. S. Institute, Perofrmance Standards for Antimicrobial Susceptiblity Testing. *CLSI supplement M100*, (2018).
52. A. M. Bolger, M. Lohse, B. Usadel, Trimmomatic: a flexible trimmer for Illumina sequence data. *Bioinformatics* **30**, 2114-2120 (2014).
53. A. Bankevich, S. Nurk, D. Antipov, A. A. Gurevich, M. Dvorkin, A. S. Kulikov, V. M. Lesin, S. I. Nikolenko, S. Pham, A. D. Prjibelski, A. V. Pyshkin, A. V. Sirotkin, N. Vyahhi, G. Tesler, M. A. Alekseyev, P. A. Pevzner, SPAdes: a new genome assembly algorithm and its applications to single-cell sequencing. *J Comput Biol* **19**, 455-477 (2012).
54. A. J. Page, C. A. Cummins, M. Hunt, V. K. Wong, S. Reuter, M. T. Holden, M. Fookes, D. Falush, J. A. Keane, J. Parkhill, Roary: rapid large-scale prokaryote pan genome analysis. *Bioinformatics* **31**, 3691-3693 (2015).
55. A. Löytynoja, *Phylogeny-aware alignment with PRANK*. Multiple sequence alignment methods (Humana Press, Totowa, NJ, 2014).
56. A. Stamatakis, RAxML version 8: a tool for phylogenetic analysis and post-analysis of large phylogenies. *Bioinformatics* **30**, 1312-1313 (2014).
57. K. A. Jolley, & Maiden, M. C., BIGSdb: scalable analysis of bacterial genome variation at the population level. *BMC bioinformatics* **11**, 595 (2010).
58. L. Cheng, T. R. Connor, J. Siren, D. M. Aanensen, J. Corander, Hierarchical and spatially explicit clustering of DNA sequences with BAPS software. *Mol Biol Evol* **30**, 1224-1228 (2013).
59. G. Tonkin-Hill, J. A. Lees, S. D. Bentley, S. D. W. Frost, J. Corander, RhierBAPS: An R implementation of the population clustering algorithm hierBAPS. *Wellcome Open Res* **3**, 93 (2018).
60. S. Koren, B. P. Walenz, K. Berlin, J. R. Miller, N. H. Bergman, A. M. Phillippy, Canu: scalable and accurate long-read assembly via adaptive k-mer weighting and repeat separation. *Genome Res* **27**, 722-736 (2017).
61. R. Vaser, Sović, I., Nagarajan, N., & Šikić, M., Fast and accurate de novo genome assembly from long uncorrected reads. *Genome research*, (2017).

62. J. Krumsiek, R. Arnold, T. Rattei, Gepard: a rapid and sensitive tool for creating dotplots on genome scale. *Bioinformatics* **23**, 1026-1028 (2007).
63. R. R. Wick, M. B. Schultz, J. Zobel, K. E. Holt, Bandage: interactive visualization of de novo genome assemblies. *Bioinformatics* **31**, 3350-3352 (2015).
64. T. Seemann, Prokka: rapid prokaryotic genome annotation. *Bioinformatics* **30**, 2068-2069 (2014).
65. A. Carattoli, E. Zankari, A. Garcia-Fernandez, M. Voldby Larsen, O. Lund, L. Villa, F. Moller Aarestrup, H. Hasman, In silico detection and typing of plasmids using PlasmidFinder and plasmid multilocus sequence typing. *Antimicrob Agents Chemother* **58**, 3895-3903 (2014).
66. R. R. Wick, L. M. Judd, C. L. Gorrie, K. E. Holt, Unicycler: Resolving bacterial genome assemblies from short and long sequencing reads. *PLoS Comput Biol* **13**, e1005595 (2017).
67. B. Jia, A. R. Raphenya, B. Alcock, N. Waglechner, P. Guo, K. K. Tsang, B. A. Lago, B. M. Dave, S. Pereira, A. N. Sharma, S. Doshi, M. Courtot, R. Lo, L. E. Williams, J. G. Frye, T. Elsayegh, D. Sardar, E. L. Westman, A. C. Pawlowski, T. A. Johnson, F. S. Brinkman, G. D. Wright, A. G. McArthur, CARD 2017: expansion and model-centric curation of the comprehensive antibiotic resistance database. *Nucleic Acids Res* **45**, D566-D573 (2017).
68. J. L. Dumas, C. van Delden, K. Perron, T. Kohler, Analysis of antibiotic resistance gene expression in Pseudomonas aeruginosa by quantitative real-time-PCR. *FEMS Microbiol Lett* **254**, 217-225 (2006).
69. D. G. Gibson, L. Young, R. Y. Chuang, J. C. Venter, C. A. Hutchison, 3rd, H. O. Smith, Enzymatic assembly of DNA molecules up to several hundred kilobases. *Nature methods* **6**, 343-345 (2009).

| Table 1. Summary of sequence types and β-lactamase encoding genes present in studied isolates | | | | | | | | | | | |
|---|---|---|---|---|---|---|---|---|---|---|---|
| **Species** | **Strain #** | **Patient #** | **Isolate #** | **ST** | **β-lactamase encoding genes** | **CAZ MIC*** | **CEP MIC*** | **TZP MIC*** | **ETP MIC*** | **MEM MIC*** | **Increased mapping density of β-lactamase-encoding genes** |
| *E. coli* | 1159 | 1 | A | 131 | $bla_{OXA-1}$, $bla_{CTX-M-15}$ | 4 | 2 | ≤ 4 | ≤0.5 | ≤0.25 | None |
| | 1283 | | B | 131 | $bla_{OXA-1}$, $bla_{CTX-M-15}$ | 4 | 2 | ≤ 4 | ≤0.5 | ≤0.25 | None |
| | 1860 | 4 | A | 131 | $bla_{OXA-1}$, $bla_{CTX-M-15}$ | 16 | ≥64 | 8 | ≤0.5 | ≤0.25 | None |
| | 2374 | | B | 131 | $bla_{OXA-1}$, $bla_{CTX-M-15}$ | 16 | 8 | ≥128 | ≤0.5 | ≤0.25 | $bla_{OXA-1}$ |
| | 2463 | | C | 131 | $bla_{OXA-1}$, $bla_{CTX-M-15}$ | 16 | 64 | ≥128 | ≥32 | 4 | $bla_{OXA-1}$ |
| | 2573 | | D | 131 | $bla_{OXA-1}$, $bla_{CTX-M-15}$ | ≥64 | ≥64 | ≥128 | ≥32 | 4 | $bla_{OXA-1}$ |
| | 1341 | 5 | A | 131 | $bla_{TEM-1}$, $bla_{CTX-M-14}$ | 4 | ≥64 | 64 | ≤0.5 | ≤0.25 | $bla_{TEM-1}$ |
| | 1676 | | B | 1604 | None | ≤ 1 | ≤ 1 | ≤4 | ≤0.5 | ≤0.25 | None |
| | 1787 | 6 | A | 156 | $bla_{TEM-169}$, $bla_{CTX-M-15}$ | ≥ 64 | ≥ 64 | ≥128 | ≤0.5 | ≤0.25 | $bla_{TEM-169}$, $bla_{CTX-M-15}$ |
| | 1871B | | B | 156 | $bla_{TEM-169}$, $bla_{CTX-M-15}$ | ≥ 64 | ≥ 64 | ≥128 | ≤0.5 | ≤0.25 | $bla_{TEM-169}$, $bla_{CTX-M-15}$ |
| | 1287 | 7 | A | 405 | $bla_{SHV-1}$, $bla_{CTX-M-15}$ | ≥64 | 16 | ≤ 4 | ≤0.5 | ≤ 0.25 | |
| | 1257 | | B | 405 | $bla_{OXA-1}$, $bla_{CTX-M-15}$ | 16 | 16 | 16 | ≤ 0.5 | ≤ 0.25 | No |
| | 1257A | | C | 10 | $bla_{OXA-181}$ | ≥ 64 | 16 | ≥128 | ≥ 32 | ≥ 16 | |
| | 1339 | 8 | A | 10 | $bla_{OXA-1}$, $bla_{CTX-M-15}$ | ≥ 64 | ≥ 64 | ≥128 | ≤ 0.5 | ≤ 0.25 | $bla_{OXA-1}$, $bla_{CTX-M-15}$ |
| | 1418 | | B | 2659 | $bla_{CTX-M-55}$ | 4 | 2 | ≤4 | ≤ 0.5 | ≤ 0.25 | No |
| | 1248 | 9 | A | 744 (ST10 | $bla_{CTX-M-55}$ | 16 | 2 | ≤4 | ≤ 0.5 | ≤ 0.25 | No |

| | | | | | | | | | | | |
|---|---|---|---|---|---|---|---|---|---|---|---|
| | | | | like) | | | | | | | |
| | 1562 | | B | 744 (ST10 like) | *bla*$_{CTX-M-55}$ | 16 | 2 | ≤4 | ≤ 0.5 | ≤ 0.25 | No |
| | 2315 | 10 | A | 10 | *bla*$_{CTX-M-55}$ | 16 | 2 | 8 | ≤ 0.5 | ≤ 0.25 | No |
| | 2446<br>2649 | | B<br>C | 10<br>10 | *bla*$_{CTX-M-55}$<br>*bla*$_{CTX-M-55}$ | ≥ 64<br>≥ 64 | ≥ 64<br>≥ 64 | ≥128<br>16 | ≥ 32<br>≤ 0.5 | 8<br>≤ 0.25 | *bla*$_{CTX-M-55}$<br>*bla*$_{CTX-M-55}$ |
| | EC215 | 11 | A | 131 | *bla*$_{OXA-1}$, *bla*$_{CTX-M-15}$ | ≥ 64 | ≥ 64 | 64 | ≤ 0.5 | ≤ 0.5 | *bla*$_{OXA-1}$, *bla*$_{CTX-M-15}$ |
| | 2489 | | B | 131 | *bla*$_{OXA-1}$, *bla*$_{CTX-M-15}$ | ≥ 64 | ≥ 64 | ≥128 | 4 | 1 | *bla*$_{OXA-1}$, *bla*$_{CTX-M-15}$ |
| | 746A | N/A | N/A | 405 | *bla*$_{OXA-1}$, *bla*$_{CTX-M-15}$ | 64 | ≥64 | ≥128 | ≥32 | 4 | *bla*$_{OXA-1}$ |
| *K. pneumoniae* | 3076 | 2 | A | Novel | *bla*$_{SHV-1}$, *bla*$_{TEM-1}$, *bla*$_{OXA-1}$, *bla*$_{CTX-M-15}$ | 4 | 2 | 16 | ≤ 0.5 | ≤ 0.25 | No |
| | 1927 | | B | Novel | *bla*$_{LEN}$ | ≤ 1 | ≤ 1 | ≤4 | ≤ 0.5 | ≤ 0.25 | No |
| | 1647 | 3 | A | 25 | *bla*$_{SHV-11}$, *bla*$_{TEM-1}$, *bla*$_{OXA-1}$, *bla*$_{CTX-M-15}$ | 16 | 8 | ≥128 | ≤ 0.5 | ≤ 0.25 | No |
| | 3087 | | B | 25 | *bla*$_{SHV-11}$, *bla*$_{TEM-1}$, *bla*$_{OXA-1}$, *bla*$_{CTX-M-15}$ | 16 | 8 | ≥128 | ≤ 0.5 | ≤ 0.25 | No |
| | 101 | N/A | N/A | 37 | *bla*$_{SHV-11}$, *bla*$_{TEM-1}$, *bla*$_{OXA-1}$, *bla*$_{CTX-M-15}$ | ≥64 | ≥64 | ≥128 | ≥32 | 8 | *bla*$_{OXA-1}$, *bla*$_{CTX-M-15}$ |

Abbreviations: ST = sequence type, MIC = minimum inhibitory concentration, CAZ = ceftazidime, CEP = cefepime, TZP = piperacillin-tazobactam, ERT = ertapenem, MEM = meropenem, *MIC reported in µg/mL.